REVIEW ARTICLE

Using Spheroids as Building Blocks Towards 3D Bioprinting of Tumor Microenvironment

Pei Zhuang, Yi-Hua Chiang, Maria Serafim Fernanda, Mei He*

Department of Pharmaceutics, University of Florida, Gainesville, Florida, 32610, USA

Abstract: Cancer still ranks as a leading cause of mortality worldwide. Although considerable efforts have been dedicated to anticancer therapeutics, progress is still slow, partially due to the absence of robust prediction models. Multicellular tumor spheroids, as a major three-dimensional (3D) culture model exhibiting features of avascular tumors, gained great popularity in pathophysiological studies and high throughput drug screening. However, limited control over cellular and structural organization is still the key challenge in achieving *in vivo* like tissue microenvironment. 3D bioprinting has made great strides toward tissue/organ mimicry, due to its outstanding spatial control through combining both cells and materials, scalability, and reproducibility. Prospectively, harnessing the power from both 3D bioprinting and multicellular spheroids would likely generate more faithful tumor models and advance our understanding on the mechanism of tumor progression. In this review, the emerging concept on using spheroids as a building block in 3D bioprinting for tumor modeling is illustrated. We begin by describing the context of the tumor microenvironment, followed by an introduction of various methodologies for tumor spheroid formation, with their specific merits and drawbacks. Thereafter, we present an overview of existing 3D printed tumor models using spheroids as a focus. We provide a compilation of the contemporary literature sources and summarize the overall advancements in technology and possibilities of using spheroids as building blocks in 3D printed tissue modeling, with a particular emphasis on tumor models. Future outlooks about the wonderous advancements of integrated 3D spheroidal printing conclude this review.

Keywords: 3D bioprinting; Tumor microenvironment; Spheroid

*Correspondence to: Mei He, at the Department of Pharmaceutics, University of Florida, Gainesville, Florida, 32610, USA; mhe@cop.ufl.edu

Received: September 6, 2021; **Accepted:** October 2, 2021; **Published Online:** October 21, 2021

Citation: Zhuang P, Chiang YH, Fernanda MS, *et al*., 2021, Using Spheroids as Building Blocks Towards 3D Bioprinting of Tumor Microenvironment. *Int J Bioprint*, 7(4):444. http://doi.org/10.18063/ijb.v7i4.444

1. Introduction

Cancer accounts for about 1 in every 6 deaths and is the second leading cause of deaths worldwide. In 2020, cancer was estimably affecting 18.3 million people globally, causing nearly 10 million deaths[1]. Despite the soaring investment in the development of anticancer therapeutics in past decades, positive outcomes are still far from satisfactory. The journey of an anticancer drug from lab-to-shelf could take years (~15 years): Before entering a clinical trial, drugs are heavily interrogated through required sets of *in vivo* and *in vitro* tests. However, a reliable *in vitro* model for accurate prediction of drug responses is lacking. Such shortfalls directly result in increased cost and time on developmental study, and overuse of animal models with slackening drug discovery processes. Addressing these issues requires a wide range of tumor models, including *in vivo*, *ex vivo*, and *in vitro* (two-dimensional [2D] and three-dimensional [3D]) models with various complexities, developed specifically for studying cancer pathology and progressing with anticancer therapeutics.

Various types of mouse models, including cancer cell line-derived and patient-derived tumor xenograft (PDX) models, have been generated by transplanting cell lines, or a fraction of human tumors heterotopically and/or orthotopically to immunocompromised mice. Cancer cell line-derived models fail in fully capturing the histopathological features exhibited in a clinical setting, although PDXs models largely preserves the genetic and epigenetic abnormalities of the original tumors when compared to patients in clinical trials[2]. Despite

this great potential of PDX models within an aspect of precision medicine, the outcomes were compromised by notably the insufficient relevant tissue-specific microenvironment support[3]. Often after engraftment, the stromal components in tumors undergo remodeling with embedded stromal cells which are gradually replaced by host stroma. The use of immunodeficient mice also leads to incompetent PDX models in immunotherapy-relevant studies which currently is a widespread concern[4]. Other problems, such as low engraftment rate[5], have also been frequently raised as a part of the key challenges.

On the other hand, *in vitro* models are speculated as promising platforms to interrogatively extrapolate *in vivo* conditions. 2D culture models lack cell-to-cell and cell-to-extracellular matrix (ECM) interactions rendered in 2D culture platforms, which are incompetent in recapitulating the heterogeneous features characteristically shown in the tumor microenvironment (TME). Substantial evidence has revealed that 3D culture is more physiologically relevant in comparison to planar culture[6,7]. The essential differences between cell behaviors, gene and protein expressions, and drug responses in 2D versus 3D cell culture systems are driving communal adoption of 3D culture toward more faithful and sophisticated tumor models. Thereafter, a series of 3D *in vitro* tumor models with diverse configurations and various complexities have been investigated for cancer research, drug discovery and have become a promising complimentary tool in bridging the *in vitro, in vivo,* and clinical investigations[8,9].

Spheroids have been recognized as classic 3D culture models for pathophysiological studies, which mimics the aggregation of one or multiple types of tumor and tumor tissue microenvironment relevant cells grown in suspension or in a 3D matrix. Spheroids are formed by boosting the cell-to-cell interaction while minimizing the cell-to-matrix adhesion[10]. Cells initially aggregate to form loose bonds by integrin-mediated attachment to ECM, which substantiates the upregulation of cadherin. This accumulation of cadherin on the cell membrane facilitates the compact spheroid formation[11], as opposed to individual cells, spheroids possess an non-apical cell morphology with stronger cell-to-cell, and cell-to-ECM interactions. Spheroids with increased cell survival rates, higher levels of ECM proteins secretion, and a more stable morphology have been reported in comparison to 2D culture[12]. Diffusion limit (~250 μm) enables ordered gradient proliferation rates observed in a large size of spheroids over 500 μm[13], which exhibit different zones with varied cell conditions delineated by the proliferation zone in the outer layer, quiescent zone in the middle layer, and necrotic zone in the center core[11]. Cells presenting in the outer layer receive abundant oxygen and culture medium, thus displaying much higher proliferation rate and viability. In contrast, cells in the core tend to be quiescent or hypoxic due to the limited supply of oxygen and nutrient delivery[14]. On the other hand, the oxygen-depleted cells anaerobically convert pyruvate to lactic acid, in an effort to produce an acidic core within spheroids. Above-mentioned observations reflect *in vivo* features of avascular tumors, in terms of cell morphology, growing kinetics, hypoxia, metabolism, nutrient gradient, and gene expression, which represent a promising platform for a better understanding of cancer biology and drug discovery *ex vivo*.

In the past few decades, 3D bioprinting has garnered extensive attention[15-17]. 3D bioprinting possesses superior flexibility and controllability on the spatial arrangement of biomaterials and cells, which has been expansively applied to tumor-related studies including TME mimicking, tumor angiogenesis, tumor metastasis, and antitumor drug screening using individual cells and miscellaneous biomaterials[18-21]. Nevertheless, individually dispersed cells within the hydrogel matrix are insufficient in faithfully recapitulating specific disease states either indicating fibrosis or tumor propagation[22]. In contrast, spheroids could be a perfect alternative and implementable approach. Despite the high potential in building tissue constructs by combining 3D bioprinting and spheroidal assembly, 3D printing or positioning spheroids with high precision remains challenging.

Herein, we review state-of-the-art status of using spheroids for mimicking tumor tissue microenvironment and their potential as building blocks in 3D bioprinting technology. We first concisely describe the context of the TME, followed by an introduction of various methodologies for spheroid formation, including the comparison of their merits and drawbacks. We then compile contemporary literature sources, providing a compelling overview of recent progress of using spheroids as building blocks for 3D printed tissue modeling, with a particular emphasis on tumor models. Finally, we discuss the future potential and challenges on spheroid formation, 3D bioprinting and their combination thereof utilized for advancing cancer research.

2. TME

Tumorigenesis is a dynamically complicated process involving its initiation, progression, and metastasis. It is governed by not only malignant tumor cells but also the constantly interacting, surrounding stroma, which is referred to as TME[23]. During tumorigenesis, the interplay between tumor cells and associated TME, reciprocally remodeling the ECM and their subsequent competition, determines whether tumorigenesis proceeds[24]. The TME is a highly heterogeneous, stage- and localization- dependent, and individually specific to its origination[25]. Only a small fraction of the tumor is comprised of tumor cells, while the larger,

non-tumor fraction houses stromal cells mainly including fibroblasts and myofibrolasts, adipocyte, blood and lymphatic vascular networks, infiltrating immune cells, and the non-cellular ECM[23], as shown in **Figure 1**. The major cell types in TME include immune cells, stromal cells, and tumor endothelial cells (TECs). Immune cells such as macrophages, dendritic cells (DCs), myeloid-derived suppressor cells (MDSCs), CD4/CD8 T cells, and regulatory T cells (Tregs) play a key role in tumor immune evasion[26]. These immune cells in TME present the resistance to immunosurveillance which recognizes and destroys foreign pathogens. Moreover, tumor-associated macrophages (TAMs) also promote angiogenesis and metastasis by producing multiple cytokines, including vascular endothelial growth factor A (VEGF-A), tumor necrosis factor α (TNFα), and interleukin 6 (IL-6)[24]. Stromal cells, including cancer-associated fibroblasts (CAFs), mesenchymal stromal cells (MSCs), and pericytes contribute to the structure of TME and promote growth, invasion, as well as metastasis of tumors. MSCs in TME, a kind of multipotent progenitor cells, can differentiate into multiple connective tissues to exacerbate tumor desmoplasia, proliferation, and angiogenesis[27]. Pericytes, along with endothelial cells, act as a physical barrier involving basement membrane remodeling during tumor angiogenesis and tumorigenesis. In addition, pericytes also regulate leukocytes transmigration and elicit phagocytic activity[28]. In addition, TECs, with irregular shape and size, build up the inner layer of blood vessels of the tumor and involve in tumor angiogenesis, progression, metastasis, and chemo drugs resistance[29]. Through providing a leaking vascular system, impaired blood flow, as well as a high-interstitial-fluid-pressure, hypoxia, and acidic environment, the disorganized TECs are key factors of tumor progression[24]. The ECM is a 3D network of extracellular macromolecules composed of collagen, laminin, fibronectin, hyaluronan, proteoglycan, and other biopolymers with varied concentrations and organizations (**Figure 1**); therefore, the ECM exists in various elasticities and dimensional stiffness.

It is well documented that stiffness of tumor is higher than that of the normal tissue and will vary across tumor grade[30]. On tissue damage, an increasing number of CAFs are detected within the tumor. These myofibroblasts are thought to be "activated" fibroblasts and will engage to promote the tumor progression[31]. Specifically, breast tumor has shown a stiffer microenvironment (4 kPa) compared to the healthy breast tissue (150~200 Pa). In

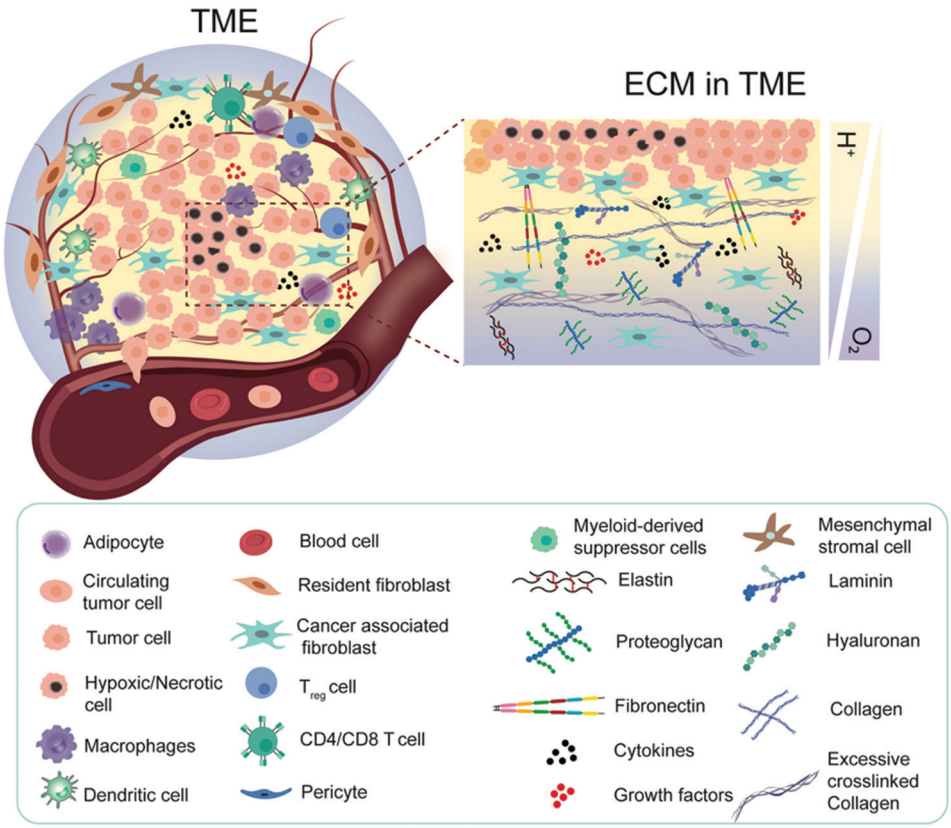

Figure 1. A schematic view of cellular components and extracellular matrix compositions of tumor microenvironment (TME). TME not only houses tumor cells but also includes stromal cells and infiltrating immune cells. Limited perfusion and tumor expansion establish a gradient of oxygen availability from the blood vessels to the adjacent tumor cells in the acidic environment.

addition, both the stroma surrounding the tumor and the tumor vasculature exhibit increased stiffness (E = ~800 – 1000 Pa and ~450 Pa, respectively) compared with healthy mammary tissue and vasculature (E = ~200 Pa) [32]. Similarly, healthy brain tissue has extremely low stiffness, typically range from 100 to 1000 Pa, whereas the increased secretion and remodeling of fibrous ECM proteins in tumor niche leads to increased tissue stiffness up to 26 kPa[33].

Hypoxia is recognized to be one of the hallmarks of the malignant tumors[34]. As tumor cells expand, the oxygen transportation to cells in the central zone is compromised due to the fact that the diffusion limit of oxygen in tissue is about 250 μm[35]. Hence, the increased metabolic rate in the external cell proliferating region and the limited access to oxygen in the core establish a gradient of oxygen availability from the blood vessels to the adjacent tumor cells. Hypoxia-inducible factor (HIF-) 1 plays a pivotal role in regulating oxygen homeostasis within cells. The hypoxic tumor cells with the upregulation of HIF-1 strive to secret VEGF, fibroblast growth factor (FGF), and other proangiogenic factors to recruit endothelial cells and facilitate capillary network formation, which is also referred to as "tumor angiogenesis"[36]. However, due to the perturbed cell-to-cell and cell-to-ECM interactions and remodeled ECM, the tumor blood vessels are chaotic and highly differed from normal host vascular network. Such leaky and highly disorganized neovasculature leads to limited oxygen diffusion and are in correlation with the ability of tumor invasion and metastasis. In the process of tumor metastasis, tumor cells travel through a series of microenvironment with changing matrix stiffness, including stroma, circulating system, endothelium, and finally the tissues at a secondary site[37].

3. Spheroid generation methods

Spheroids have found great potential in anticancer pharmaceutical development, because they are able to resemble the main features of humanoid tumors in many aspects; for instance, structural organization, and metabolic and proliferative gradients[13]. A spheroid's size could be tailored to specific applications. In general, cellular types, seeding density, and culture period are working synergistically in appropriating the size of spheroids. Uniformity of the spheroids is of utmost importance because the relevant size and shape dictate therapeutic efficacy and clinical reproducibility. Numerous strategies have been reported in attempting to form spheroids with desired size and uniformity, including hanging drop[38-40], agitation-based techniques[41,42], liquid overlay technique (LOT)[43], hydrogel microwells[44,45], external-force-driven (magnetic, electric, acoustic) techniques[46-48], microfluidics[49,50], and 3D bioprinting[51] (**Figure 2**).

3.1. Hanging drop technique

Hanging drop technique is a straightforward and well-established method for spheroid preparation, which is also the most frequently used method, due to its ease in handling and user-friendliness without needs of specialized instrumentation. Briefly, small droplets of cells are deposited on a lidded surface of a polystyrene tissue culture plate (**Figure 2A-a**).

Driven by gravity, cells in the droplet start to aggregate and eventually form spheroids at the bottom of the droplets[52]. By adjusting the diameter of the contact area (3, 5 and 7 mm) and droplet volume (10 – 153 μL), Gao *et al*. have developed a hanging drop platform with controlled geometry to investigate the effects of droplet curvature, spreading area and cell density on spheroid formation using β-TC-6 islet cells. These results demonstrated that at a fixed volume, the radius of drop curvature was proportional to the diameter of the guiding circle, and a small radius of curvature yielded spheroids with better aggregation and compactness. A guiding circle with a selected diameter of 5 mm exhibited the highest efficient spheroid formation. The selected cell density of 105 cells/mL gave rise to spheroids with a diameter of 400 – 500 μm, which was well aligned with native islet size[53]. Notably, the optimized spheroids made of islet cells exhibited similar morphology and function to primary islets as compared to 2D culture, which indicates the superior role of 3D culture.

Optimizations were conducted and reported on these hanging drop methods for promoting spheroid formation[38]. Due to a higher hydrophobic nature and a selected droplet contact angle of 99°, polydimethylsiloxane (PDMS) was demonstrated to be superior to polystyrene in generating more uniformly compacted spheroids[52]. Notably, the supplement of collagen fibril at 500 μg/ml in the hanging droplet greatly accelerated the spheroid formation within 24 h. In addition, other additives, such as poly (N-isopropylacrylamide) and methylcellulose, have also been promising in aiding uniformly compact spheroid formation[54,55]. Industrial scale-up strategies regarding the manufacturing of spheroids in a high-throughput manner are reported (**Figure 2A-a$_1$**). A hanging drop spheroid culture array plate that could give rise to up to 384 spheroids had been developed[39,40]. These corresponding results displayed that the osmolality could be maintained at a desired culture range, requiring 30% of culture medium exchanged every other day. Taken together, the hanging drop method displays excellent control on the size and shape of spheroids, yet is unstable and laborious. Medium exchange as well as the drug administration can be time-consuming and challenging. Inappropriate practice might disturb the spheroids and result in a compromised integrity. Moreover, accurate monitoring of growth with regard to the spheroids, in real-time, is difficult to achieve.

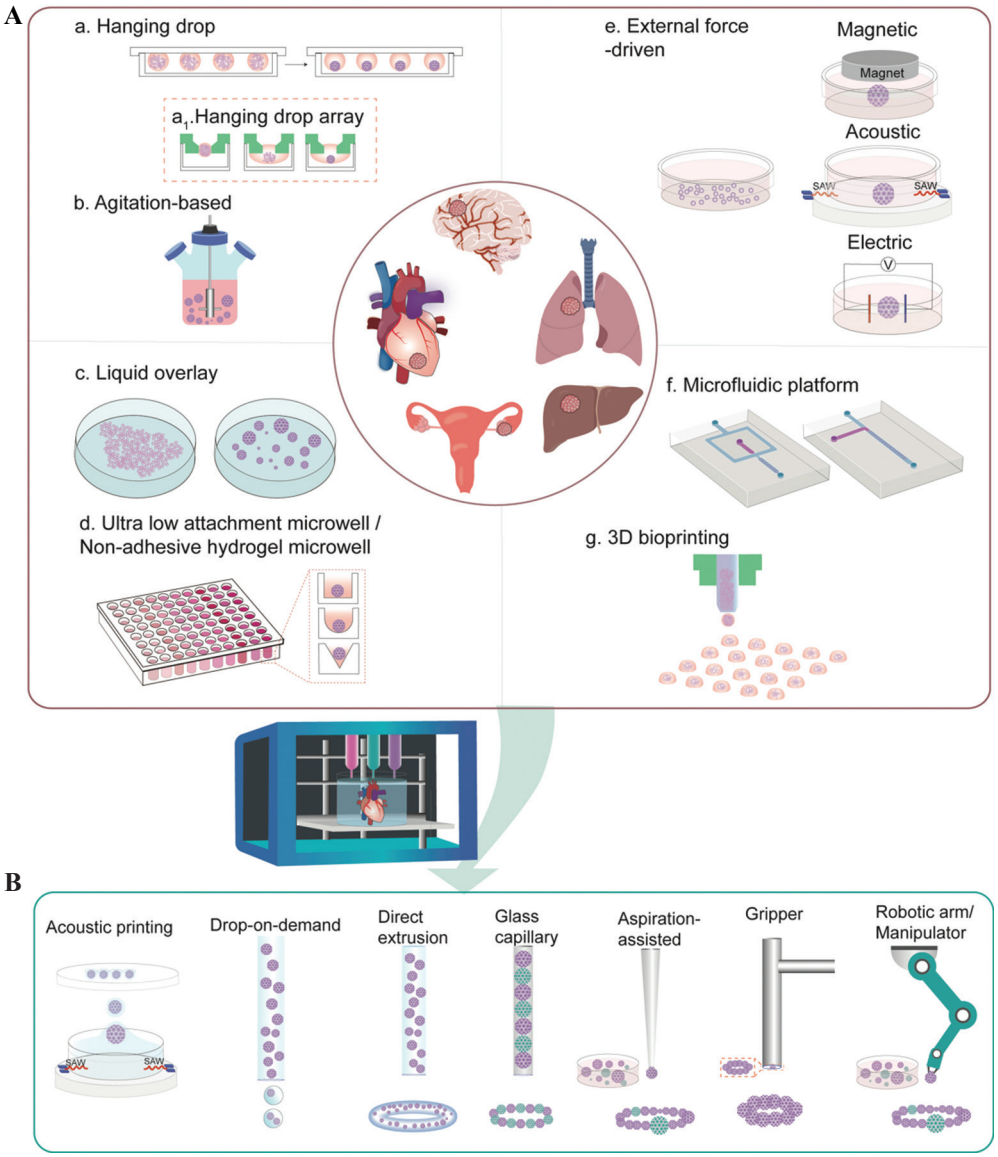

Figure 2. Schematic illustration of using spheroids as building blocks in 3D bioprinting for healthy/disease tissue construction. (A) Overview of spheroid formation techniques. (B) 3D Printing and its adaptions in assisting spheroid assembly.

3.2. Agitation-based methods

Agitation-based methods promote spheroid formation by maintaining cells in suspension using specialized equipment, such as spinner flasks, roller bottles, gyratory shakers, or a NASA bioreactors through continuous stirring by an impeller(s) or magnetic stirrer(s)[41,56-59]. This approach enables mass production of spheroids with long-term culture, while also allows tracking of these spheroids during constant culture (**Figure 2A-b**). In particular, using a bioreactor facilitates the control over pH, oxygenation and nutrient concentration[60]. However, these spheroids are generated in a single compartment, resulting in poor control over size and uniformity. The stirring rate and the culture time need to be constantly monitored. The combined stirrer's mechanical stress coupled with the fluid's shear stress generated from the high stirring rate may cause cell damage and reduce the spheroid formation, whereas a low stirring rate may not be able to prevent cell sedimentation.

3.3. LOT

Different from agitation-based technique (subjecting cells to high shear stress), LOT is a static technique that suspends cell culture on non-adhesive surfaces, prevents cell-to-substrate adhesion, and promotes cell-to-cell interaction, advantageously with low shear stress (**Figure 2A-c**). Typically, this non-adhesive surface is achieved by pre-coating with biocompatible materials such as agarose[61-63] and poly-2-hydroxyethyl methacrylate (polyHEMA)[64-66]

on any commercially available cell culture plate. Among them, agarose is the most widely utilized material due to its cost-effectiveness and ease of handling. Agarose could be simply prepared, sterilized by autoclave, and solidified in only a few minutes after coating. In addition, polyHEMA is recognized as an effective alternative for spheroid formation. Briefly, a homogeneous polyHEMA solution can be obtained by dissolving polyHEMA powder in 95% ethanol at 65°C overnight, followed by a drying process at room temperature and ethanol evaporation at temperature up to 37°C. The drying process could take days to weeks according to different protocols[66-68]. Regardless of the preparation time, polyHEMA solutions can be stored at 4°C for up to 2 months[68], whereas agarose solution cannot be lengthily stored because repeated heating impairs the properties of agarose.

Like agitation-based techniques, spheroids generated by LOT on flat surfaces are revealed as irregularly shaped and disorganized. Optimizations have been attempted in increasing amenability to high-throughput applications. Ivascu *et al*. had conducted a systematic parametric study about optimal spheroid formation on polyHEMA-coated surface in terms of cell types, cell density, medium additives, plate type (round bottom and conical shaped bottom), and the presence of horizontal stirring[69]. Twenty tumor cell lines of different lineages were examined. A series of medium additives with varied concentrations have been systematically screened for optimal spheroid formation, including reconstituted basement membrane (rBM), collagen type I and type IV, laminin, fibronectin, heparan sulphate proteoglycan and chondroitin sulphate. Interestingly, the results reported the compact spheroid formation for all the cell lines with the addition of 2.5% rBM. In addition to ECM-related components, methylcellulose is also validated as an additive support for compact, unisized spheroid formation[70].

3.4. Non-adhesive hydrogel microwell

Micro-molded microwells using non-adhesive hydrogels have been proven as an effective alternative for spheroid formation. Similar to the LOT, non-adhesive materials are used in preventing cell adhesion to the bottom of the microwell. A series of materials have been explored, such as agarose[71], polyethylene glycol diacrylate (PEGDA)[72], and PDMS[73]. Among them, agarose is most prevalently used for micro-molding[74-76]. Briefly, a microfeature mold is fabricated through soft lithography or rapid prototyping, a PDMS-negative replicate could be achieved subsequently. Thereafter, the agarose micro-mold could be obtained by casting into the PDMS replicate[75]. Micro-molds with an array of various patterns, for instance, flat surface or a conical shape with a rounded bottom and hemispherical shape, have been demonstrated in promoting spheroid formation (**Figure 2A-d**)[75,77]. Evidenced by their successful fabrications of micro-molded non-adhesive agarose hydrogels composed of 822 concave recesses (800 μm deep × 400 μm wide)[78], this technique is relatively high throughput with effortless scale up capabilities. Spheroid growth becomes easily accessible during culture. In contrast to the hanging drop method, cell medium change and drug administration are more convenient to accomplish without the risk of disturbing the spheroids using LOT and non-adhesive hydrogel microwells.

3.5. External force-driven methods

External forces, such as electromagnetic and acoustic forces, have been applied in generating spheroids (**Figure 2A-e**). The utilization of dielectrophoresis (DEP), in the development of multicellular aggregation, was successfully demonstrated and optimized[48]. DEP functions by producing an external force on a dielectric particle when it is subjected to a non-uniform electric field, analogous to piezoelectric materials. Cells could be guided by dielectrophoretic forces to form clusters; however, the clusters could be damaged by mechanical or hydrodynamic forces after the removal of electric field. Hence, a range of biomaterials, including but not limit to collagen, PEGDA, agarose, pluronic, and PuraMatrix, have been introduced for immobilizing and stabilizing the cell aggregates[79-81].

Magnetized cells could be obtained by cell internalization. Magnetic nanoparticles, including magnetoferritin, superparamagnetic iron oxide nanoparticles and its cousin, gold, could be internalized into cell cytoplasm through endocytosis, or by surface functionalization[82]. As an example of surface functionalization, magneto-functionalized cell membrane was readily achieved with a combination of poly-L-lysine mixed gold or iron oxide nanoparticles[83]. Leveraging this newly embedded magnetic capability, magnetized cells could be levitated and agglomerated to form spheroids when magnets are placed on the culture dish or using a magnetic lid[46,82,84]. Spheroids formed with magnetized cells demonstrated a negligible adverse effect on cell viability while accelerating spheroidization time. Diverse structures and sizes of 3D cellular aggregates could be achieved through the adjustment a magnetic field configuration[85]. Urbanczyk *et al*. have investigated the interaction of pancreatic β-cells with vascular endothelial cells in heterotypic pancreatic spheroid models using magnetic levitation in three different configurations. The results identified that human umbilical vein endothelial cells (HUVECs), which disassembles from the spheroids over time, spontaneously formed spheroids, highlighting this significant role of magnetic levitation. Magnetic levitation could enhance the stability of heterotypic spheroids, facilitating HUVEC integration[83].

Integrating acoustics with microfluidics and acoustic fluidics have found many applications in cell sorting and separation[86]. This acoustic-based cell manipulation technique is non-invasive and label-free. By guiding surface acoustic waves (SAW) to a microfluidic chamber, Chen *et al*. had demonstrated spheroid formation, while simultaneously patterning through a designed 3D acoustic tweezer platform[47]. Guo *et al*. had developed a high-throughput acoustic fluidic platform for large-scale spheroid formation[87]. By acoustically assembling cancer cells, this platform enables high throughput fabrication of 6000 tumor spheroids per batch within 24 h.

3.6. Microfluidic platforms

By manipulating fluid flow between micro- and nano-scales within microchannels, microfluidic platforms have evolved as powerful tools that could possibly miniaturize significant experimental processes onto a microfluidic chip less than the size of a finger[88]. Droplet-based microfluidics, which generates discrete droplets via immiscible multiphase flows inside microfluidic devices, have gained substantial interest in past decades. Through adjustments to the flow rate of immiscible fluids, this method enables generation of highly monodispersed droplets with a production speed spanning from 10-1000 droplets per second[89]. Typically, there are 3 types of microfluidic configurations for passive droplet generation: cross-flowing/T junction[90,91], flow-focusing[92-95], and co-flowing droplet formation[96]. Flow-focusing with single-, double-, and multiple-emulsion designs have been extensively utilized (**Figure 2A-f**)[97-99]. As a result, cell-encapsulated capsules with a template of water-in-oil (w/o), oil-in-water-in-oil (o/w/o), water-in-water-in-oil (w/w/o), and water-in-oil-in-water (w/o/w) could be produced[100,101]. By assigning different materials and/or cells to replace each individual phase, microcapsules displaying varied cell/material arrangements could be tailored for diverse applications[102]. For instance, with a double-emulsion, flow-focusing microfluidic device, Agarwal *et al*. had developed core-shell microcapsules with embryonic stem cell-laden carboxymethyl cellulose and alginate in the core and shell, respectively. Other than alginate[98], hydrogels such as chitosan, thermosensitive gelatin, agarose, Matrigel, collagen, P(NIPAM-AA), photoinitiative gelatin methacrylate (gelMA), PEGDA, and hyaluronic acid-MA have all been examined for facilitating spheroid formation and growth[94]. In addition to droplet-based microfludics, lab-on-a-chip technology also can integrate hanging drop networks[103-105], microwell[50,106], U-shape microstructure, or micropillar into the platforms for spheroid formation and on-chip culture. Microfluidic platforms outperform conventional static culture methods through the introduction of a perfusion flow that could improve oxygen and nutrient transportation, sustaining long-term cell culture[107,108].

These continuous flow-based microfluidic platforms frequently use and require syringe pumps, whereas digital microfluidic platforms can optimally dispense pico- to micro-liter droplets on an electromechanical apparatus; therefore, digital microfluidic platform are more portable and cost-effective[109-111]. Through tight control over fluidic flow, microfluidic platforms allow the generation of monodispersed droplets with uniform spheroid formation coupling a high throughput production output[112,113].

3.7. 3D Bioprinting techniques

Despite the broad utilization of extrusion-based bioprinting in building 3D tissue constructs, strong interests in inkjet-based bioprinting have been growing substantially in recent decades. The capability of a "drop-on-demand" style printing to accurately dispense discrete spheroids makes this technique appealing for high-throughput spheroid formation (**Figure 2A-g**). By dispensing the cell droplets into an alginate hydrogel matrix residing within a 96-well plate, through microvalve-based printing, Utama *et al*. had successfully generated spheroids using 3 different cell types, including neuroblastoma (SK-N-BE(2)), non-small cell lung cancer (H460), and glioblastoma (U87vIII) cells[114]. The size of these printed spheroids was controlled by adjusting the initial printing cell density and incubation time, as well as the confinement of the printed hydrogel matrix. Evidenced by the expression of Ki67, HIF-1α, and apoptotic marker cleaved caspase-3, the 3D-printed SK-N-BE(2) spheroids exhibited similar tumor-like characteristics that resemble manually formed spheroids. Similar level of CD133 expression was found in both 3D printed and manually generated neuroblastoma spheroids, indicating a similar preservation of cancer stemness between both types of spheroids. Therapeutic efficacy was also examined by doxorubicin (DOX) treatment for 2 h. DOX penetration was found on the periphery of both types of prepared spheroids, which are also frequently observed in tumors. These results collectively demonstrated the capability of 3D printed spheroids in recapitulating the biological features of tumors.

Taking advantage of the thermal property of gelatin hydrogel, Ling *et al*. had fabricated concave wells molded from a polyethylene glycol-dimethacrylate (PEG-DMA) array, with *in situ* seeding of human breast cancer cell-laden gelatin for cellular spheroid formation on a chip[115]. However, challenges associated with droplet inconsistency, low cell density, easy nozzle blockage, and physical stresses on cells limit the range of this technique's applicability. Alternatively, laser-based bioprinting also enables droplet-based printing for single cell manipulation or 3D spheroid formation[116,117].

Using the platform, laser direct-write, Kingsley *et al*. had generated size and shape controllable chitosan-shelled alginate structures with human breast cancer cells and mouse embryonic stem cells encapsulated, respectively[51]. Adjusting the beam diameter of the laser enables control over the printed aggregate sizer ranging from 200 μm and 400 μm. These obtained microbeads were further washed in chitosan solution, forming a core-shell structure that could constrain the aggregate geometry. Over a 14-day culture period, both cells showed high cell viability. Notably, both cell types self-assembled into 3D aggregates to match the corresponding geometry of their printed constructs. Similarly, with the laser-assisted bioprinting, Hakobyan *et al*. had created 3D pancreatic cell spheroid arrays using the AR42J-B-13 rat acinar cell line for studying the initial stages of pancreatic ductal adenocarcinoma development[118]. The printed spheroids were observed with a diameter around 30-40 μm. Taken together, this nozzle-free, laser-assisted method allows spheroid generation with a high resolution and density, but rather financially taxing in usage[115]. In addition, although extrusion-based bioprinting is not as capable in generating droplets, they have been utilized to print 3D microtissue inserts[119], or hanging drippers[40], availing toward a high-throughput spheroid formation.

4. 3D printing-assisted spheroid assembly

Despite the great efforts that have been devoted to 3D-printed TME, the progress is limited by many reasons including the incompliant mechanical stiffness of the bio-inks and thus compromised cell-to-cell, cell-to-ECM interactions. Spheroid is recognized as a physiologically relevant 3D model that could capture the key characteristics of both healthy and disease tissues. Given the high cell density, increased deposition of ECM and accelerated proliferation rate, spheroids-based model could greatly reduce the tissue maturation time. Such densely packed spheroid is thus proposed as building blocks for either healthy or diseased tissue modeling. However, the spheroid growth and fusion are highly disorganized, which would ultimately affect the consistency in therapeutic outcomes. To impose spatial control and guide the spheroid fusion and arrangement, several strategies such as direct fusion and magnetic-driven assembly have been explored for manipulating spheroids. However, major issues, such as poor positioning resolution, simple structures, and the requirement of specialized instruments, are yet to be addressed. Given the capability of bioprinting in spatial control, several 3D printing strategies and its adaptions have been investigated for their potentiality in spheroid assembly. The software programs for converting digital files to real 3D printing can be as complex as AutoCAD and SolidWorks or 3ds Max and Maya, or as simple as TinkecCAD or OpenSCAD. G-code is the standard program used by outputting from slicing software and setting instructions for 3D printers to move the stage and printer nozzles in x-, y-, and z-axes along with bio-ink extrusion.

Finally, the embedded software that runs on the printer itself takes the G-code and turns it into electrical signals for running various motors. This is usually done in C/C++ but could also be written in anything that fits on the printer's hardware.

4.1. Direct extrusion-based printing

Swaminathan *et al*. investigated the bioprinting of pre-formed breast epithelial spheroids in alginate-based bio-ink co-culture with endothelial cells[120,121], and demonstrated that the printed pre-formed spheroids exhibited high cell viability and maintained their spheroid morphology after bioprinting, either in monoculture or co-culture with HUVECs. Moreover, the 3D-printed spheroids were shown to be more resistant to the paclitaxel treatment as compared to 3D-printed individual cells, highlighting that the spheroids have preserved their function after being extruded. This study has validated the capability of printing spheroids directly using extrusion-based bioprinting. To maintain the integrity and avoid spheroid aggregation in printing cartridge and nozzle clogging, the size of the spheroids was confined to ~70 μm.

Recently, Horder *et al*. have interrogated the interaction between adipose-derived stromal cell (ASC) and breast cancer cells in a 3D-printed co-culture model[122]. The model was composed of directly printed ASC spheroids in hyaluronic acid (HA)-rich hydrogel. The printability of ASC spheroids (228 ± 22 μm) was assessed using 2 different needle sizes, 250 and 330 μm, with a corresponding pressure at 5 bar and 1 bar. Printing with the 330 μm needle caused 9% damage on the integrity of the printed spheroids, while the damage and cell death was dramatically increased to 56% using the 250 μm needle. Over a 21-day differentiation culture, the printed ASC spheroids showed substantial and sustained adipogenesis. Comparable levels of triglyceride, the expression of both early markers (PPAR and C/EBP) and late marker (fatty acid-binding protein 4 (FABP4)) of adipogenic differentiation, and the secretion of adiponectin were demonstrated in both printed and non-printed spheroids, indicating that the printing process have negligible effects on the cellular differentiation. Evidenced by Oil Red O staining and quantitative analysis of intracellular triglycerides, a considerable reduction on lipid content in co-culture constructs was observed as compared to ASCs monoculture model. Moreover, the immunostaining for the major ECM components collagen I, IV, and VI, laminin, and fibronectin revealed the ECM remodeling in the co-culture model. These features reflected what was observed *in vivo*, highlighting

the physiological relevance of the printed co-culture model. Taken together, extrusion-based printing enables the direct spheroid printing without any modification to the printing setup. However, the resolution of extrusion-based printing is needle size-dependent, thus limiting the size and density of the spheroids. The integrity of large spheroids will be compromised, and the high spheroid density is liable to induce nozzle blockage.

Interestingly, utilizing a capillary micropipette with a defined diameter at 300 or 500 μm in bio-printer, Jakab *et al*. have successfully delivered multicellular spheroids to collagen type I substrate and formed certain structures, such as ring, sheets, and cylinders[123]. Interestingly, the spheroids were formed by a rapid centrifugation, incubation, and a cutting process to secure the size consistency in obtained spheroids. The spheroids were then aspirated into a capillary micropipette as a printing cartridge and extruded from the cartridge through the positive displacement of a piston within the micropipette. This printing technique was subsequently applied to engineer vessels of distinct shapes and hierarchical trees with diameters spanning from 900 μm to 2.5 mm. Agarose was used as temporary support to facilitate the construction of hanging features. The deposited discrete spheroids underwent post-printing fusion and formed single-layer and double-layer tubular structures. Notably, with the adapted capillary micropipette as printing cartridge, this scaffold-free approach circumvents some shortcomings associated with exogeneous biomaterials and provides much better control over the spheroid geometry and position, therefore greatly improving the reproducibility and scalability as compared to the non-adapted extrusion-based printing.

4.2. Droplet-based bioprinting

Apart from extrusion-based printing, other bioprinting modalities such as microvalve-based printing[124], laser-assisted printing[125], and acoustic printing[126] have also been explored for their capability in printing spheroid aggregates. By adopting an open cartridge, Chen *et al*. introduced a nozzle-free, contact-free acoustic-driven bioprinting that allows both cell and spheroid ejection[126]. Cell encapsulating GelMA droplets were ejected onto a receiving substrate in a pre-designed arrangement, followed by UV crosslinking that stabilizes the structure. The authors had generated a co-culture TME with the tumor spheroid in the central zone and the CAFs in the periphery. Over a 7-day culture period, increased tumor spheroid invasion area and distance was observed in co-culture model as compared to monoculture, suggesting that CAFs may promote morphological changes within tumor cells. Such a nozzle-free printing approach holds great potential for constructing tissue models with low cell damage, although the resolution is limited and only suitable for bio-inks with low viscosity. This method alleviates heat or mechanical damage exerted by the bioprinting nozzle on the cells/spheroids, enabling printing with high cell densities (>10^8 cells/mL).

4.3. Kenzan method

Proposed by Prof. Koich Nakayama, Kenzan method has been frequently used in constructing tissue models with scaffold-free bio-inks. Kenzan, which is also referred to as a microneedle-based method, using stainless-steel needle arrays that function as temporary support for spheroids and allow the *in-situ* fusion of the spheroids to form a macro-tissue[127]. The spheroids are picked up by a mobile nozzle arm from well plates and moved on the top of the microneedle array. By switching the negative pneumatic pressure to slightly positive, the spheroids are released into the substrate. The process is repeated until the entire construct is completed and left on the microneedle array for continuous culture.

Upon fusion, the needle arrays are retracted, and the obtained tissue could be perfused and cultured for further maturation[128,129]. Kenzan method has found its application in many tissues, including blood vessel, tracheal, heart, liver, and urinary bladder[130]. In a seminal study, van Pel *et al*. investigated glioma cell invasion into neural-like tissues using Kenzan method[131]. Eight neurospheres formed from induced pluripotent stem cells (iPSC)-derived human neural progenitor cells were robotically placed in the micro-needle arrays and cultured for 3 weeks for fusion and maturation into a neural organoid. U118 human glioma cell spheroids were subsequently printed on the top of the neural organoid and cultured for up to 4 weeks. Revealed by cryosectioning and confocal imaging, GFP^+ U118 cells were found within the human neural organoid, which confirmed the glioma cell invasion. However, no gliosis was observed surrounding the tumor or invading cells, which was different from the previous observations. In summary, the Kenzan method has greatly facilitated the scaffold-free fabrication from various cell types into complex structures, particular tubular constructs but the fixed distance between needles (~400 μm) requires the size-consistent spheroids with a diameter approximate to ~600 μm to ensure their direct contact with one another[132], which significantly restrains the size of usable spheroids and highly relys on spheroid preparation, especially when a large quantity of spheroids is needed. Besides, the mechanical interruption could induce the structural damage to the spheroids, particularly the smaller ones.

4.4. Gripper and manipulator

In addition, gripper or micromanipulator has also been introduced to assemble the spheroids. Notably, inspired by electronics manufacturing, an instrument named Bio-Pick, Place, and Perfuse (Bio-P3) was introduced

to assist the large-scale tissue block translocation[133,134]. Using polycarbonate track-etched membrane-integrated cell culture inserts as the gripper and a peristaltic pump to generate fluid suction through the nozzle's membrane, the nozzle could pick-up, transfer and release the spheroids/microtissues with minimized damage to the living cells, while perfusing the parts in an aqueous environment. As a proof-of-concept, a series of features including spheroids, toroids, and honeycombs with sizes range from 600 μm to 3.4 mm was created to validate the capability of the instrument. A stack of 16 donut ring constructs and 4 honeycombs have been successfully assembled and fused over a 48 h-period for culture to form a single tissue[134]. In a lateral study, the optimization on the system enabled the stacking of 20 honeycomb-shaped structures with improved alignment accuracy[133]. Such strategies have offered an effective alternative for assembling spheroids as building blocks, though with limited precision and prolonged fabrication period.

4.5. Aspiration-assisted bioprinting (AAB)

Harnessing the strength of aspiration forces, Ayan *et al*. have developed an AAB technique that enables to pick and print spheroids with a broader range of sizes from 80 μm to 600 μm in a high precision manner. The printer was adapted from a low-cost commercial printer and equipped with a custom-made tapered pipette (diameter ~80 μm)[135]. Coupling with conventional micro-valve printing, the spheroids could be either printed on hydrogel-based substrate or without scaffold. To demonstrate the capability of the printing strategy, spheroids with different viscoelastic surface tension properties and varied size ranges from 200-600 μm were prepared from a wide range of cell types, including HUVECs, mouse fibroblast cell line (3T3), mouse mammary carcinoma line (4T1), human mesenchymal stem cells (MSCs), HUVECs/MSCs, and human dermal fibroblasts. A heterogeneous pyramid construct was printed using spheroids with different sizes and types, indicating that the technique allows the printing of non-uniform spheroids. The printing accuracy was reported to be ~11% with respect to the spheroid size. The printed spheroids exhibited an overall moderate viability over 80%. Further, in combination with Freeform Reversible Embedding of Suspended Hydrogels (FRESH) printing, they have further extended the versatility of AAB by precisely positioning spheroids in self-healing yield-stress hydrogels to achieve more complicated tissue structures[136]. Both Carbopol with varied concentrations at 0.8%, 1.2%, 1.6% and 0.5% alginate microparticles were investigated for their potentiality as supporting bath for spheroids printing using AAB in terms of positional accuracy and cell viability post printing. As demonstrated, the positional accuracy for 0.8%, 1.2%, and 1.6% concentrations of Carbopol and alginate microparticles were ~97%, 22%, 12%, and 34%, respectively. Notably, over a 3-day culture period, spheroids cultured in 1.2% Carbopol showed a reduced viability around 74%, while maintaining a 93% survival rate in alginate microparticles. Similarly, Daly *et al*. have also printed spheroids in a modified HA-enriched hydrogel supporting bath with a ~10% with respect to spheroid size positional precision[137]. Conclusively, the AAB technique offered an effective alternative to position spheroids in a highly reproducible and precise fashion, therefore giving rise to reliable and robust 3D *in vitro* models for disease modeling. The overall reported methods for generating spheroids were summarized in below **Table 1**.

5. Progress in establishing 3D tumor models via 3D bioprinting

Conventional 3D models, such as spheroids and scaffold-based constructs, offer limited control over cell organization and ascribe poor vascularization. Such shortfalls leave us with oversimplified tumor models, which are incompetent for understanding tumor biology and fail to predict accurate therapeutic response. In recent years, 3D bioprinting technology has undergone rapid development and evolution[141]. The outstanding spatial control over cells and materials, coupled with an integration of vascular networks into the platform, could give rise to higher fidelity 3D tumor models with greatly increased complexity.

To date, bioprinting technologies can be categorized into extrusion-based[142], inkjet-based[143], laser-based[144], and stereolithography techniques[145]. Each technique has its own merits and drawbacks and requires bio-inks with specific properties[146-148]. Indeed, the critical role of bio-inks is embedding a mechanical property that regulates the cellular response. Particularly, in extrusion-based bioprinting, the major stumbling block is the imbalance of printability and the mechanical property of the selected bio-ink[149]. With the development of FRESH printing, where a semisolid suspension bath is used to print into, the resolution of printing intricate hierarchical features such as vascular networks could be significantly improved. Furthermore, this newfound capability of generating soft matrices from low viscous bio-ink provides excitingly tailorable elicitations of any desired cellular response, thus boosting the cell proliferation[150]. Through the aid of bioprinting technologies, a variety of 3D printed models have been created, producing significant advances toward mimicking *in vivo* tumor structure and cell growth behavior as summarized in **Figure 3**. Accumulating studies were reported, describing the use of 3D bioprinting platforms with increased complexity and key features for mimicking tumor progression in an architecturally relevant manners, such as tumor heterogeneity[151-154], tumor angiogenesis[155-157], metastasis[158-160], and anti-

Table 1. 3D printing assisted spheroid assembly

Printing strategy	Target tissue	Spheroid generation method	Materials	Cell type (density)	Spheroid size/ spheroidization time (ST)/ fusion time (FT)	Feature	Ref
Extrusion-based printing	Breast cancer	Falcon 8 chamber polystyrene vessel	Matrigel, gelatin-alginate, collagen-alginate	MCF10A, MCF10A-NeuN, MDA-MB-231, MCF7	5000 cells/well Size~100 μm ST: MCF10A cells, 8–10 d; MCF-7, MDA-MB-231, MCF10A-NeuN, 5–6 d FT: N.A.	• High cell viability in mono- and co-culture • More resistant to paclitaxel than individual cells • Size limitation of spheroid • Limited control over spheroid arrangement	[121]
Extrusion-based printing	Breast cancer	8-well chamber slide	Matrigel	MCF10A MDA-MB-231 (10000 cells/well) HUVECs	Size<70 μm ST: MCF10A, 8 d; MDA-MB-231, 5 d FT: N.A.	• MDA-MB-231 migrates out of spheroids in co-culture with HUVECs • Limited control on bioprinted spheroid location and number • Size limitation of spheroid	[120]
Extrusion-based bioprinting	Breast cancer	Agarose molds cast in MicroTissues®3D Petri Dishes®	Thiol-modified HA, unmodified high concentration HA,	ASCs (2500 cells/ spheroid) MDA-MB-231	4800 spheroids/mL Size: 228 ± 22 μm ST: 2 d FT: N.A.	• Reduction of the lipid content • Increased fibronectin, collagen I and collagen VI expression • Limited control over spheroid arrangement • Size limitation of spheroid	[122]
Extrusion-based printing (capillary micropipette)	Cardiac tissue	Pellet centrifugation	Collagen type I (Bio-paper)	Cardiac and endothelial cells, VEGF	Size: 300/500 μm ST: A few minutes FT: 70 h	• Synchronously beating after 90 h • Size-consistent spheroids • Weak spheroids	[123]

(Contd...)

Table 1. *(Continued)*

Printing strategy	Target tissue	Spheroid generation method	Materials	Cell type (density)	Spheroid size/ spheroidization time (ST)/ fusion time (FT)	Feature	Ref
Extrusion-based printing (capillary micropipette)	Vascular	Pellet centrifugation	Agarose as temporary support	Chinese Hamster Ovary cell, Human umbilical vein smooth muscle cells, Human skin fibroblasts, porcine aortic smooth muscle cells	Size: 300/500 μm ST: 1-2 h FT: 5-7 d	• Size consistent spheroids • Long fusion time • Large quantity of spheroids preparation is time consuming • Non-uniform structure • Weak spheroids	[138]
Multifunctional Fabion 3D bioprinter with the turnstile system	Thyroid gland	Hanging drop	Collagen	Individual thyroid explants and allantoides	Size: thyroid, 388.2 μm±45.3; Allantoide, 493.6 μm±114.3 ST: 18-24 h	• Turnstile allows the deposition of spheroid one at a time • Improved vascularization	[139]
Scaffold-free bioprinter/ Regenova/kenzan method	Glioblastoma	96-well U-bottom plates	N.A.	iPSC-derived human neural progenitor cells (40,000 cells/well), U118 human glioma cells (10,000 cells/well)	Size: 500 μm ST: 48 h FT: 3 weeks	• Mechanical damage to the integrity of spheroids • Fixed spacing between needles • High cost	[131]
Aspiration-assisted bioprinting	Post-myocardial infarction (MI) scarring	Ultra-low attachment 96-well round-bottom plates	HA modified with either adamantane (Ad) or β-cyclodextrin (CD)	Human MSCs, Human cardiac fibroblasts Human iPSC-CM	Size: 5000 cells/200 μm 10000 cells/400 μm ST: 96h FT: 4d	• High resolution positioning (~10% spheroid size) • High density micro-tissue • High cell viability	[137]
Aspiration-assisted bioprinting	/	U-bottom 96-well microplate	Fibrin	3T3, mouse mammary carcinoma line 4T1, HUVECs/MSCs, HDF, electrocytes 2500-10,000 cells/ well	80-800 μm (~30 s/spheroid) ST: 24h	• ~11%with respect to the spheroid size --position accuracy • Non-uniform spheroids printing	[135]

(Contd...)

Table 1. *(Continued)*

Printing strategy	Target tissue	Spheroid generation method	Materials	Cell type (density)	Spheroid size/ spheroidization time (ST)/ fusion time (FT)	Feature	Ref
Aspiration-assisted bioprinting	Osteogenic tissues, cartilage	96-well plate	Carbopol, alginate microparticles	Human MSC spheroids	Osteogenic spheroid, 20000 cells/well; chondrogenic spheroids, 50000 cells/well	• Alginate microparticles: ~34% positional accuracy	[136]
Bio-P3 instrument	Tumor	Nonadhesive agarose micro-mold	N.A.	Rat hepatoma (H35), human ovarian granulosa (KGN), human breast cancer (MCF-7) cells	1250 cells/ spheroid feature, 25,000–40,000 cells/toroid feature, and 250,000 cells/ honeycomb feature ST: spheroid and toroids, 18-24 h; honeycomb, 48 h FT: 48 h	• Allow large microtissue pick-up • Manually operated • Long fabrication time • Limited gripper size available • Optical clarity required	[134]
	Hepatoma	Nonadhesive agarose micro-mold	N.A.	HepG2	375 000 cells/ honeycomb mold ST: 24 h	• Syringe pump-better flow control • Allow large part pick-up • Long fabrication time • Optical clarity required	[133]
Micro-manipulator	/	Non-adhesive round-bottom 96-well plate	N.A.	NIH/3T3 spheroids	3000 cells/well	• Spheroid size >300 μm	[140]
Microvalve printing	Breast cancer	Culture in Matrigel for 7 days (0.5 million cells/mL)	Elastin-like protein-RGD hydrogels	Human premalignant breast epithelial cells (MCF10ATs) spheroid	~ 50 μm	• Maintained morphology and size	[124]
Laser direct-write	Breast cancer	High-voltage electric field-driven microbead fabrication	Alginate/collagen Alginate/gelatin	MDA-MB231, MCF-7, or mixed MDA-MB-231/ MCF-7 breast cancer cells	Size: 300–400 μm	• Real-time video monitoring • Microbead shifting • Limited resolution	[125]
Acoustic droplet printing	Oral cancer	Hanging-drop method	GelMA	Oral squamous cell carcinoma (OSCC) cell line CAL27 spheroids, CAF	600 cells/spheroid, Size ~ 150 μm	• Nozzle-free • Contact-free • Low cell damage	[126]

cancer drug screening[161,162]. Those notable reports also detailed the challenges of current existing technologies for assembling cell-favorable biomaterials with multiple cell types in complex tissue microenvironment as we summarized in **Figure 3**.

Using spheroids as building blocks in facile macro-sized tissue construction has been proposed[163], the most straightforward method in assembling these spheroids is spontaneous fusion[164-167]. Fleming *et al*. had reported a spheroidal fusion between unilluminated vascular spheroids through liquid-like coalescence. Specifically, 2 juxtaposed spheroids were fused when positioned close enough, forming a larger spheroid with preserved composite structural characteristics[168]. These features have legitimized a notion of suitability for using spheroids as building modules in engineering large-scale tissues for tissue regeneration and/or disease modeling. Early studies have also demonstrated the feasibility of assembling spheroids through directed fusion, achieving microtissues with prescribed patterns including honeycomb, rods, and tori[169,170]. Briefly, spheroids are manually placed in a pre-designed mold/template containing the prescribed topography. These spheroids will then gradually fuse together and achieve the specified pattern over time. This manual processing has shed light on a great possibility of generating tissue constructs by spheroidal modular assembly, despite its limited control and low throughput. For overcoming such challenge, several bioengineering strategies have been exploited for spheroid assembly, potentiating its large-scale functional tissue manufacturing with improvements in accuracy through a high-throughput manner.

Leveraging magnetic force, spheroids that are functionalized with magnetic nano/microparticles can be assembled into specific patterns by imposing temporary magnetic fields[171-176]. An applied magnetic field could accelerate the cell aggregation process, but the topology of the constructs is highly dependent on the magnetic template[172,173]. In addition, the association of magnetic particles is inevitable, and the linker involved may engender safety issues. The effects of magnetic nanoparticles on cell physiology and function, other than fundamental cell viability and proliferation, should be considered before further involvement. Instead of magnetically labeling cells, an alternative usage is paramagnetizing the cells. Alahough a paramagnetic

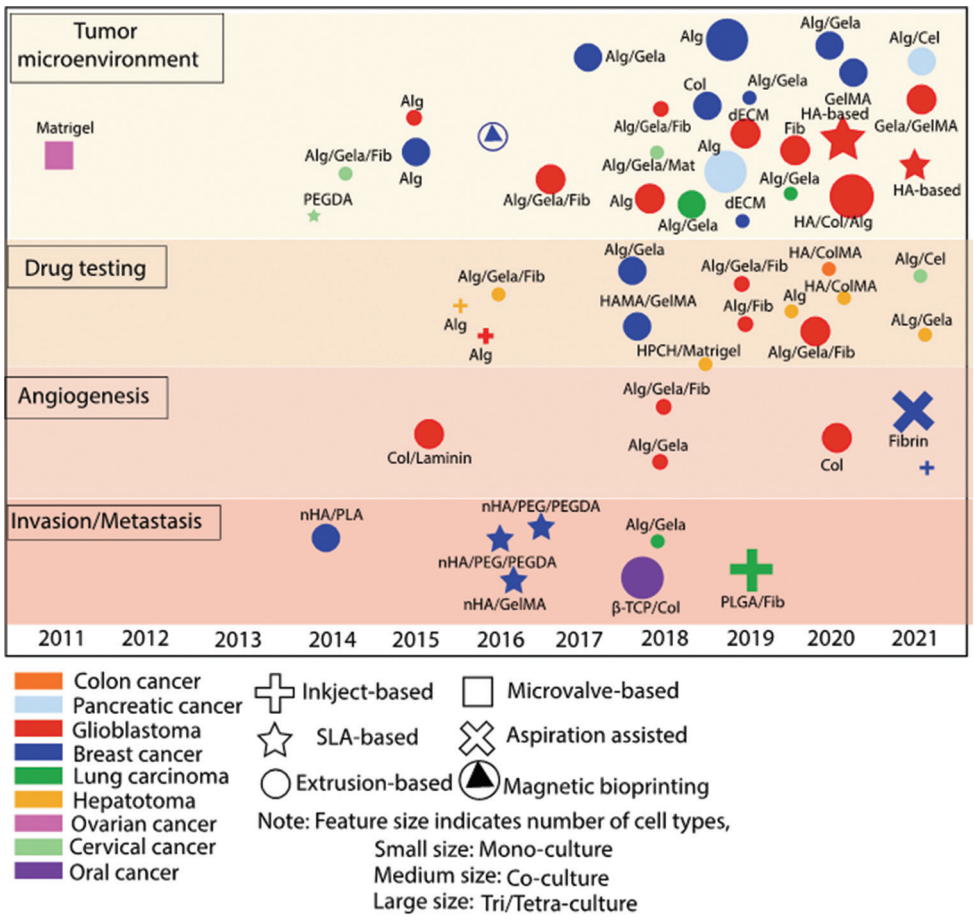

Figure 3. Progress in establishing 3D tumor models via 3D bioprinting.

agent could be removed after spheroidal construction, these paramagnetic agents, at high concentration, could be detrimental to cell survival. Comparatively, another label-free alternative using acoustic wave has also been investigated. By applying non-destructive SAW, Chen *et al*. assembled large amounts of cell spheroids in a fluidic environment, forming various patterns within a couple of seconds[177]. By altering the acoustic wave frequency, several geometric patterns ranging from circle, square, and line to complex geometries could be obtained. A complete fusion of fibroblast spheroids, HUVEC spheroids, and co-cultured spheroids were observed within 72h. To explore this versatility and modularity, the selected strategy was further applied to generate densely packed hepatic tissue constructs from fibroblast, HUVECs and primary rat hepatocytes. Notably, the formation of bile canaliculi was observed at the hepatic junctions over a 6-day culture. The results highlighted a remarkable effectiveness of this contactless, biocompatible, and label-free method in assembling spheroids through a highly efficient process. Interestingly, Parfenov *et al*. recently reported a hybrid magnetoacoustic bioassembly method that allowed rapid assembly of 3D tissue construction from spheroids within a medium, with a relatively low concentration of paramagnetic agent (gadolinium salt)[178]. Harnessing the strength from both magnetic waves and acoustic sounds, this method not only circumvents a challenge from a potentially adverse effect stemming from the paramagnetic agent, but also imparts more flexibility on the assembled structure.

The major challenge associated with replicating tumor models is simulating the heterogeneity of cellular components and ECM. Dynamic interactions between cells and the ECM contribute to tumor initiation, progression, and metastasis through biophysiochemical cues. For instance, macrophages are a heterogeneous population of cells that are crucial to the detection, phagocytosis, and destruction of pathogens. However, when recruited to tumor cells, the TAMs polarize differently and do not display an anti-inflammatory role but rather facilitate tumor growth and angiogenesis. In understanding the crosstalk between glioblastoma cells and macrophages, Heinrich *et al*. generated a 3D-bioprinted mini-brain with GelMA/gelatin encapsulating mouse glioblastoma cells (GL261) in the core of a mouse macrophage cell line (RAW264.7)-enriched at the peripheral[179]. Over a 4-day culture, active migration of macrophages toward tumor cells was observed, while tumors also displayed migration behavior toward macrophages, albeit less dramatic, indicating that macrophages could be actively recruited by tumor cells and polarized into a Glioblastoma-associated macrophages (GAMs) specific phenotype.

Another notable study on interrogating the functional dependencies and cellular interactions in the brain tumor was conducted by Tang *et al*. They developed a 3D-printed glioblastoma (GBM) model consisting of patient-derived glioblastoma stem cells (GSCs), astrocytes, and neural stem cells (NSCs), with or without the presence of macrophages in a blended GelMA and glycidyl methacrylate-HA hydrogel through digital light processed-based bioprinting[180]. The printed construct was composed of 2 regions: (i) GSC or mixed GSC/macrophage encapsulated tumor cores, (ii) surrounded by a non-neoplastic region enriched with NSCs and astrocytes. The upregulation of the glioblastoma tissue-specific gene sets, as compared to 2D and GSC spheres, suggested a better dynamic viewing window of transcriptional states than *ex vivo*-derived glioblastoma tissues. Further, the inclusion of macrophages resulted in upregulation of hypoxic response and glycolic metabolism, eliciting invasiveness signatures in the tetra-culture brain tumor model. This significantly indicated that the 3D-printed GBM model, to a higher extent, resembled the pathologic conditions *in vivo*.

The TME comprises numerous signaling molecules and resulting pathways that influence the angiogenic response. Achieving a durable and efficient antiangiogenic response will require approaches that simultaneously and/or sequentially target multiple aspects of the TME[181]. Dey *et al*. developed a 3D-vascularized breast cancer micro-environment that consists of HUVECs, metastatic MDA-MB-231 cells, and fibroblasts-laden fibrin gel as the tumor stroma to investigate the interactions between cellular and acellular components in a TME[182]. Given the critical role of matrix stiffness in regulating tumorigenesis, matrix density affecting angiogenesis and invasion was investigated by varying the fibrinogen and thrombin concentration. The impact of fibroblasts was examined by embedding the pre-vascularized spheroids into a fibrin matrix, which was pre-loaded with fibroblasts in a serial density from 0.25 million to 2 million cells/mL. Interestingly, an increase in total vessel length and branching index was observed with increasing fibroblast densities ranging from 0.25 million to 1 million cells/mL, indicating enhanced angiogenesis. Furthermore, to mimic a vascularized TME, HUVECs were introduced into the fibrin matrix with fibroblasts in a 2:1 ratio to create a vascular bed for tumor cells. Over a 7-day culture period, HUVECs that sprouted from the laden tumor spheroid anastomosed with the vascularized fibrin matrix, organizing into a wide range of capillaries. Cancer cells were observed within capillary networks, indicating their intravasation. Taken together, these multicellular bioprinted tumor models, with exquisite control on both cellular and acellular components, serving as promising platforms to interrogate cellular crosstalk, cell-to-

ECM, as well as tumor-immune interactions in a more physiologically relevant microenvironment.

Recent progress in bioprinting techniques, biomaterial science and cell biology have generated 3D tumor models with greatly enhanced robustness and physiological relevance. Such models with higher fidelity hold great potential not only in unraveling the underlying mechanism, but also facilitating the anticancer drug screening before entering clinical trials. For instance, to validate the reliability of the printed co-culture platform in the above-mentioned study[183], immunotoxins EGF4KDEL and CD22KDEL which target EGFR-overexpressing A549s and an off-target parallel control, respectively, were introduced through the vascular conduit. Specifically, EGF4KDEL greatly suppressed the tumor growth, invasion, and migration, while negligible effect was observed with the treatment of CD22KDEL. By interlacing cancer cells, stromal cells, and vascular networks, this bioprinted model was reminiscent of the native TME, providing a valuable reference for anticancer drug screening. Similarly, several models displaying varied complexities have been constructed for anticancer drug testing[184-187]; yet, the majority were utilizing animal cells or immortal human cell lines, which could be less effective in therapeutic prediction. Notably, in a recently published study, Xie *et al*. generated a patient-derived hepatocellular carcinoma (HCC) model using cell-laden gelatin/alginate as bio-ink[188]. Immunofluorescence staining revealed the stabilized expression of α-fetoprotein in HCC model over a 2-week culture period. In addition, evidenced by whole-exome sequencing and RNA-sequencing; a high level of concordance for single nucleotide variants was observed between 3D printed HCC model and the corresponding original HCC tissue, indicating the retained genetic alterations and expression profiles. Overall, the results demonstrated that the 3D-printed HCC model could preserve the features of the original tumor during long-term culture. The printed models were subsequently subjected to the treatments with 4 commonly used, dose-dependent targeting drugs. The patient-specific response suggested the potentiality of the 3D-printed model as a drug prediction model for personalized medicine.

6. Outlooks and challenges

TME is now recognized as a highly dynamic and heterogeneous environment with reciprocal interactions between cellular and acellular components. Although massive efforts have been dedicated to emulating the key features of TME, the majority of these studies are focusing on a single aspect within TME, i.e. a true-to-life tumor model. This golden model could recapitulate all the essential characteristics of TME, but currently, its construction is restricted by technological limitations. Given its potentiality in recapitulating the key features of the avascular tumor *in vivo*, spheroids have been identified as a promising tool for understanding tumor biology and anticancer therapeutic development. However, the random structural organization yields inconsistent therapeutic outcomes, which greatly precludes the model from translational clinical applications. Featuring with excellent control system, bioprinting has been greatly beneficial to the tissue engineering field. The existing 3D printed models are serving as promising platforms, providing deeper insights into some critical aspects of tumor progression, including but not limited to tumor heterogeneity resemblance, tumor angiogenesis, metastasis, and anticancer therapeutic development. However, the major issue in the current 3D printed models is balancing the mechanical properties of exogeneous bio-inks with the biological functions of sportingly involved cellular components. To this end, there is a growing interest in adopting spheroids as building blocks within 3D bioprinting, possibly achieving large-scale tissue construction. Harnessing the power from spheroids and 3D bioprinting would likely circumvent associated shortcomings from using foreign bio-inks (mismatched mechanical stiffness and degradation rate, etc.), while maintaining structural guidance for spheroid growth. Therefore, tumor models with increased authenticity, including well-organized structure, maximized cell-to-cell interaction, cell-secreted ECM, and multicellular environment, could be fabricated in a high-throughput manner. Although, promising progresses have been achieved in 3D printing spheroids so far, current existing technologies could not accurately position the spheroids. In addition, spheroid processing (including spheroidization, assembly process, tissue fusion, and maturation) is time consuming. Using spheroids as tissue building blocks in 3D bioprinting is still in its infancy.

Conventional spheroid generation strategies have offered wealthy information on parameters that affect spheroid formation but are not scalable. For instance, 96-well U bottom well plate are very expensive, and worsens when a large amount of spheroids are required -a large amount of spheroids require more 96 well plates, which is very expensive[189]. Recent advent of microfluidic platforms and drop-on-demand bioprinting are promising on improving the high throughput fabrication of spheroids, yet the spheroid uniformity is far from satisfactory. New methods, such as machine learning, bring emerging solutions by integrating imaging and screening of functional modules into the current systems for spheroid selection through morphological feature analysis. A fully automated system can significantly improve the fabrication performance and lessen the time. Lee *et al*. integrated a machine learning model using least general generalization algorithm combined with

yield stress, viscoelasticity, and shape fidelity from using various type I collagen-based bio-inks[190]. By separating the class variables into shape fidelity and extrusion, the machine learning algorithm effectively optimized the composite bio-ink material fraction and subsequent printing performance[191,192]. Current applications of 3D bioprinting based machine learning algorithms are currently geared towards using regressive models such as LASSO; however, a potential avenue of integrating advanced learning systems using generative ensembles or Bayesian approaches in producing highest performing inks of spheroidal assembly remains completely untapped. Current existing technologies are challenged by spheroid precision positioning coupled with an assembly process lasting tediously for a simple structure, not even including the spheroid production and the post-printing tissue maturation. Apart from technical improvements on the printer, biomaterials such as nanofibers, nanoparticles, hydrogels could be designed and incorporated, and could instruct accelerated spheroidal formative growth and tissue maturation. Scaffold-free spheroid printing could overcome the shortcomings of exogeneous biomaterials, while functional bio-inks with appropriate mechanical property hold great potential to improve the position accuracy. Further, vascular networks and lymphatic systems are essential components that are associated with tumor angiogenesis and metastasis. To present a strong reminiscence of the native TME, both blood vessels and lymphatic vessels should be involved. Co-cultured spheroids have also been generated from various types of cells, such as fibroblast and HUVECs, to replicate the complexity of the tissue microenvironment[13,193,194]. Particularly, in the presence of endothelial cells, capillary-like network formations have been achieved by co-cultured spheroids. Moor *et al*. had generated tri-cultured spheroids composed of HUVECs, human foreskin fibroblasts and adipose tissue-derived MSCs using a non-adhesive agarose microwell, and reported optimized culture ratio and cell density through which endothelial cells underwent self-sorting and formed capillary-like networks within these spheroids[195]. Prospectively, prevascularized spheroids could serve as promising building units for fabricating large-scale tissue models that require proper vascularization[196]. In addition, the incorporation of printing with sacrificial material or in supporting bath to create hollow channels for vascularization would likely help to achieve better vascularization. Notably, adopting the sacrificial writing into functional tissue approach, Skylar-Scott *et al*. created perusable vascular networks in the organ building blocks' bath through embedded 3D bioprinting[189]. The great potential of 3D bioprinting is harnessing a strategy to print patient-specific human tissues with patient-derived cells. Future works focusing on using patient-derived cells are likely to provide deeper insights into the stage-dependent, patient-specific tumor cell behavior, further elucidating tumor progression dynamics, and thus facilitating stronger anticancer therapeutic development.

Acknowledgments

The authors would like to thank funding support by NIH NIGMS MIRA award 1R35GM133794 to Dr. Mei He

Conflicts of interest

The authors declare no conflict of interest.

References

1. Sung H, Ferlay J, Siegel RL, *et al*., 2021, Global Cancer Statistics 2020: GLOBOCAN Estimates of Incidence and Mortality Worldwide for 36 Cancers in 185 Countries. rtd*CA Cancer J Clin*, 71:209–49. https://doi.org/10.3322/caac.21660.
2. Jackson SJ, Thomas GJ, 2017, Human Tissue Models in Cancer Research: Looking Beyond the Mouse. *Dis Model Mech*, 10:939–42. https://doi.org/10.1242/dmm.031260
3. Yoshida GJ, 2020, Applications of Patient-derived Tumor Xenograft Models and Tumor Organoids. *J Hematol Oncol*, 13: 4. https://doi.org/10.1186/s13045-019-0829-z
4. Goto T, 2020, Patient-Derived Tumor Xenograft Models: Toward the Establishment of Precision Cancer Medicine. *J Pers Med*, 10:64. https://doi.org/10.3390/jpm10030064
5. Lai Y, Wei X, Lin S, *et al*., 2017, Current Status and Perspectives of Patient-derived Xenograft Models in Cancer Research. *J Hematol Oncol*, 10:106. https://doi.org/10.1186/s13045-017-0470-7
6. Ozturk MS, Lee VK, Zou H, *et al*., 2020, High-resolution Tomographic Analysis of *In Vitro* 3D Glioblastoma Tumor Model under Long-term Drug Treatment. *Sci Adv*, 6:eaay7513. https://doi.org/10.1126/sciadv.aay7513
7. Rijal G, Li W, 2017, A Versatile 3D Tissue Matrix Scaffold System for Tumor Modeling and Drug Screening. *Sci Adv*, 3:e1700764. https://doi.org/10.1126/sciadv.1700764
8. Ferreira LP, Gaspar VM, Mano JF, 2018, Design of Spherically Structured 3D *In Vitro* Tumor Models Advances and Prospects. *Acta Biomater*, 75:11–34. https://doi.org/10.1016/j.actbio.2018.05.034

9. Stock K, Estrada MF, Vidic S, *et al*., 2016, Graeser, Capturing Tumor Complexity *In Vitro*: Comparative Analysis of 2D and 3D Tumor Models for Drug Discovery. *Sci Rep*., 6:28951. https://doi.org/10.1038/srep28951
10. Laschke MW, Menger MD, 2017, Life is 3D: Boosting Spheroid Function for Tissue Engineering. *Trends Biotechnol*, 35:133–44. https://doi.org/10.1016/j.tibtech.2016.08.004
11. Cui X, Hartanto Y, Zhang H, 2017, Advances in Multicellular Spheroids Formation. *J R Soc Interface*, 14:20160877. https://doi.org/10.1098/rsif.2016.0877
12. Achilli TM, Meyer J, Morgan JR, 2012, Advances in the Formation, Use and Understanding of Multi-cellular Spheroids. *Expert Opin Biol Ther*, 12:1347–60. https://doi.org/10.1517/14712598.2012.707181
13. Nunes AS, Barros AS, Costa EC, *et al*., 2019, 3D Tumor Spheroids as *In Vitro* Models to Mimic *In Vivo* Human Solid Tumors Resistance to Therapeutic Drugs. *Biotechnol Bioeng*, 116:206–26. https://doi.org/10.1002/bit.26845
14. Edmondson R, Broglie JJ, Adcock AF, *et al*., 2014, Three-dimensional Cell Culture Systems and their Applications in Drug Discovery and Cell-based Biosensors. *Assay Drug Dev Technol*., 12:207–18. https://doi.org/10.1089/adt.2014.573
15. Zhuang P, Sun AX, An J, *et al*., 2018, 3D Neural Tissue Models: From Spheroids to Bioprinting. *Biomaterials*, 154:113–33. https://doi.org/10.1016/j.biomaterials.2017.10.002
16. Zhuang P, An J, Chua CK, *et al*., 2020, Bioprinting of 3D *In Vitro* Skeletal Muscle Models: A Review. *Mater Des*, 193:108794. https://doi.org/10.1016/j.matdes.2020.108794
17. Shin YJ, Shafranek RT, Tsui JH, *et al*., 2021, 3D Bioprinting of Mechanically Tuned Bioinks Derived from Cardiac Decellularized Extracellular Matrix. *Acta Biomater*, 119:75–88. https://doi.org/10.1016/j.actbio.2020.11.006
18. Ma X, Liu J, Zhu W, *et al*., 2018, 3D Bioprinting of Functional Tissue Models for Personalized Drug Screening and *In Vitro* Disease Modeling. *Adv Drug Deliv Rev*, 132:235–51. https://doi.org/10.1016/j.addr.2018.06.011
19. Kang Y, Datta P, Shanmughapriya S, *et al*., 2020, 3D Bioprinting of Tumor Models for Cancer Research. *ACS Appl Bio Mater*, 3:5552–73. https://doi.org/10.1021/acsabm.0c00791
20. Zhang YS, Duchamp M, Oklu R, *et al*., 2016, Bioprinting the Cancer Microenvironment. *ACS Biomater Sci Eng*, 2:1710–21. https://doi.org/10.1021/acsbiomaterials.6b00246
21. Albritton JL, Miller JS, 2017, 3D Bioprinting: Improving *In Vitro* Models of Metastasis with Heterogeneous Tumor Microenvironments. *Dis Model Mech*, 10:3–14. https://doi.org/10.1242/dmm.025049
22. Tang M, Rich JN, Chen S, 2021, Biomaterials and 3D Bioprinting Strategies to Model Glioblastoma and the Blood Brain Barrier. *Adv Mater*, 33:2004776. https://doi.org/10.1002/adma.202004776
23. Wang M, Zhao J, Zhang L, *et al*., 2017, Role of Tumor Microenvironment in Tumorigenesis. *J Cancer*, 8:761–73. https://doi.org/10.7150/jca.17648
24. Baghban R, Roshangar L, Jahanban-Esfahlan R, *et al*., 2020, Tumor Microenvironment Complexity and Therapeutic Implications at a Glance. *Cell Commun Signal*, 18:59. https://doi.org/10.1186/s12964-020-0530-4
25. Winkler J, Abisoye-Ogunniyan A, Metcalf KJ, *et al*., 2020, Concepts of Extracellular Matrix Remodelling in Tumour Progression and Metastasis. *Nat Commun*, 11:5120. https://doi.org/10.1038/s41467-020-18794-x
26. Anderson NM, Simon MC, 2020, The Tumor Microenvironment. *Curr Biol*, 30:R921–R925. https://doi.org/10.1016/j.cub.2020.06.081
27. Cuiffo BG, Karnoub AE, 2012, Mesenchymal Stem Cells in Tumor Development: Emerging Roles and Concepts. *Cell Adh Migr*, 46:220–30. https://doi.org/10.4161/cam.20875
28. Ribeiro AL, Okamoto OK, 2015, Combined Effects of Pericytes in the Tumor Microenvironment. *Stem Cells Int*, 2015:868475. https://doi.org/10.1155/2015/868475
29. Nagl L, Horvath L, Pircher A, *et al*., 2020, Tumor Endothelial Cells (TECs) as Potential Immune Directors of the Tumor Microenvironment New Findings and Future Perspectives. *Front Cell Dev Biol*, 8:766. https://doi.org/10.3389/fcell.2020.00766
30. Wullkopf L, West AK, Leijnse N, *et al*., 2018, Cancer Cells' Ability to Mechanically Adjust to Extracellular Matrix Stiffness Correlates with their Invasive Potential. *Mol Biol Cell*, 29:2378–85. https://doi.org/10.1091/mbc.E18-05-0319
31. Kalli M, Stylianopoulos T, 2018, Defining the Role of Solid Stress and Matrix Stiffness in Cancer Cell Proliferation and Metastasis. *Front Oncol*, 8:55. https://doi.org/10.3389/fonc.2018.00055
32. Bahcecioglu G, Basara G, Ellis BW, *et al*., 2020, Breast

Cancer Models: Engineering the Tumor Microenvironment. *Acta Biomater*, 106:1-21. https://doi.org/10.1016/j.actbio.2020.02.006

33. Wang C, Sinha S, Jiang X, *et al*., 2021, Matrix Stiffness Modulates Patient-Derived Glioblastoma Cell Fates in Three-Dimensional Hydrogels. *Tissue Eng Part A*, 27:390–401. https://doi.org/10.1089/ten.TEA.2020.0110
34. Muz B, de la Puente P, Azab F, *et al*., 2015, The Role of Hypoxia in Cancer Progression, Angiogenesis, Metastasis, and Resistance to Therapy. *Hypoxia* (*Auckland, NZ*), 3:83–92. https://doi.org/10.2147/HP.S93413
35. Vajda J, Milojević M, Maver U, *et al*., 2021, Microvascular Tissue Engineering a Review. *Biomedicines*, 9:589. https://doi.org/10.3390/biomedicines9060589
36. Chen L, Endler A, Shibasaki F, 2009, Hypoxia and Angiogenesis: Regulation of Hypoxia-inducible Factors Via Novel Binding Factors. *Exp Mol Med*, 41:849–57. https://doi.org/10.3858/emm.2009.41.12.103
37. Peela N, Truong D, Saini H, *et al*., 2017, Advanced Biomaterials and Microengineering Technologies to Recapitulate the Stepwise Process of Cancer Metastasis. *Biomaterials*, 133:176–207. https://doi.org/10.1016/j.biomaterials.2017.04.017
38. Oliveira MB, Neto AI, Correia CR, *et al*., 2014, Superhydrophobic Chips for Cell Spheroids High-Throughput Generation and Drug Screening. *ACS Appl Mater Interfaces*, 6:9488–95. https://doi.org/10.1021/am5018607
39. Tung YC, Hsiao AY, Allen SG, *et al*., 2011, High-throughput 3D Spheroid Culture and Drug Testing Using a 384 Hanging Drop Array. *Analyst*, 136:473–8. https://doi.org/10.1039/c0an00609b
40. Zhao L, Xiu J, Liu Y, *et al*., 2019, A 3D Printed Hanging Drop Dripper for Tumor Spheroids Analysis Without Recovery. *Sci Rep*, 9:19717. https://doi.org/10.1038/s41598-019-56241-0
41. Massai D, Isu G, Madeddu D, *et al*., A Versatile Bioreactor for Dynamic Suspension Cell Culture. Application to the Culture of Cancer Cell Spheroids. *PLoS One*, 11:e0154610. https://doi.org/10.1371/journal.pone.0154610
42. Franchi-Mendes T, Lopes N, Brito C, 2021, Heterotypic Tumor Spheroids in Agitation-Based Cultures: A Scaffold-Free Cell Model That Sustains Long-Term Survival of Endothelial Cells. *Front Bioeng Biotechnol*, 9:447. https://doi.org/10.3389/fbioe.2021.649949
43. Costa EC, de Melo-Diogo D, Moreira AF, *et al*., 2018, Spheroids Formation on Non-Adhesive Surfaces by Liquid Overlay Technique: Considerations and Practical Approaches. *Biotechnol J*, 13:417. https://doi.org/10.1002/biot.201700417
44. Lee JM, Park DY, Yang L, *et al*., 2018, Generation of Uniform-sized Multicellular Tumor Spheroids Using Hydrogel Microwells for Advanced Drug Screening. *Sci Rep*, 8:17145. https://doi.org/10.1038/s41598-018-35216-7
45. Tu TY, Wang Z, Bai J, *et al*, 2014, Rapid Prototyping of Concave Microwells for the Formation of 3D Multicellular Cancer Aggregates for Drug Screening. *Adv Healthc Mater*, 3:609–16. https://doi.org/10.1002/adhm.201300151
46. Kim JA, Choi JH, Kim M, *et al*, 2013, High-throughput Generation of Spheroids Using Magnetic Nanoparticles for Three-dimensional Cell Culture. *Biomaterials*, 34:8555–63. https://doi.org/10.1016/j.biomaterials.2013.07.056
47. Chen K, Wu M, Guo F, *et al*., 2016, Rapid Formation of Size-controllable Multicellular Spheroids Via 3D Acoustic Tweezers. *Lab Chip*, 16:2636–43. https://doi.org/10.1039/C6LC00444J
48. Sebastian A, Buckle AM, Markx GH, 2007, Tissue Engineering with Electric Fields: Immobilization of Mammalian Cells in multilayer Aggregates Using Dielectrophoresis. *Biotechnol Bioeng*, 98:694–700. https://doi.org/10.1002/bit.21416
49. Wu Z, Gong Z, Ao Z, *et al*., 2020, Rapid Microfluidic Formation of Uniform Patient-Derived Breast Tumor Spheroids. *ACS Appl Bio Mater*, 3:6273–83. https://doi.org/10.1021/acsabm.0c00768
50. Ruppen J, Wildhaber FD, Strub C, *et al*., 2015, Towards Personalized Medicine: Chemosensitivity Assays of Patient Lung Cancer Cell Spheroids in a Perfused Microfluidic Platform. *Lab Chip*, 15:3076–85. https://doi.org/10.1039/C5LC00454C
51. Kingsley DM, Roberge CL, Rudkouskaya A, *et al*., 2019, Laser-based 3D Bioprinting for Spatial and Size Control of Tumor Spheroids and Embryoid Bodies. *Acta Biomater*, 95:357–70. https://doi.org/10.1016/j.actbio.2019.02.014
52. Kuo CT, Wang JY, Lin YF, *et al*, 2017, Three-dimensional Spheroid Culture Targeting Versatile Tissue Bioassays Using a PDMS-based Hanging Drop Array. *Sci Rep*, 7:4363. https://doi.org/10.1038/s41598-017-04718-1
53. Gao B, Jing C, Ng K, *et al*., 2019, Fabrication of Three-dimensional Islet Models by the Geometry-controlled Hanging-drop Method. *Acta Mech Sin*, 35:329–37.

https://doi.org/10.1007/s10409-019-00856-z

54. Ware MJ, Colbert K, Keshishian V, *et al*., 2016, Generation of Homogenous Three-Dimensional Pancreatic Cancer Cell Spheroids Using an Improved Hanging Drop Technique. *Tissue Eng Part C Methods*, 22:312–21. https://doi.org/10.1089/ten.TEC.2015.0280
55. Vignesh RA, Kumari S, Poddar P, *et al*., 2020, Poly(N-isopropylacrylamide)-Based Polymers as Additive for Rapid Generation of Spheroid via Hanging Drop Method. *Macromol Biosci*, 20:2000180. https://doi.org/10.1002/mabi.202000180
56. He H, He Q, Xu F, *et al*., 2019, Dynamic Formation of Cellular Aggregates of Chondrocytes and Mesenchymal Stem Cells in Spinner Flask. *Cell Prolif*, 52:e12587. https://doi.org/10.1111/cpr.12587
57. Shi W, Kwon J, Huang Y, *et al*., 2018, Facile Tumor Spheroids Formation in Large Quantity with Controllable Size and High Uniformity. *Sci Rep*, 8:6837. https://doi.org/10.1038/s41598-018-25203-3
58. Lancaster MA, Knoblich JA, 2014, Generation of Cerebral Organoids from Human Pluripotent Stem Cells. *Nat Protoc*, 9:2329–40. https://doi.org/10.1038/nprot.2014.158
59. Lei X, Ning L, Cao Y, *et al*., 2011, NASA-Approved Rotary Bioreactor Enhances Proliferation of Human Epidermal Stem Cells and Supports Formation of 3D Epidermis-Like Structure. *PLoS One*, 6:e26603. https://doi.org/10.1371/journal.pone.0026603
60. Salehi-Nik N, Amoabediny G, Pouran B, *et al*., 2013, Engineering Parameters in Bioreactor's Design: A Critical Aspect in Tissue Engineering. *Biomed Res Int*, 2013:762132. https://doi.org/10.1155/2013/762132
61. Lei KF, Lin BY, Tsang NM, 2017, Real-time and Label-free Impedimetric Analysis of the Formation and Drug Testing of Tumor Spheroids Formed via the Liquid Overlay Technique. *RSC Adv*, 7:13939–46. https://doi.org/10.1039/C7RA00209B
62. Gaskell H, Sharma P, Colley HE, *et al*., 2016, Characterization of a Functional C3A Liver Spheroid Model. *Toxicol Res* (*Camb*), 5:1053–65. https://doi.org/10.1039/c6tx00101g
63. Costa EC, Gaspar VM, Coutinho P, *et al*., 2014, Optimization of Liquid Overlay Technique to Formulate Heterogenic 3D Co-cultures Models. *Biotechnol Bioeng*, 111:1672–85. https://doi.org/10.1002/bit.25210
64. Chen YC, Lou X, Zhang Z, *et al*., 2015, High-Throughput Cancer Cell Sphere Formation for Characterizing the Efficacy of Photo Dynamic Therapy in 3D Cell Cultures. *Sci Rep*, 5:12175. https://doi.org/10.1038/srep12175
65. Kim JH, Lim IR, Joo HJ, *et al*., 2015, Sphere Formation of Adipose Stem Cell Engineered by Poly-2-hydroxyethyl Methacrylate Induces *In Vitro* Angiogenesis through Fibroblast Growth Factor 2. *Biochem Biophys Res Commun*, 468:372–9. https://doi.org/10.1016/j.bbrc.2015.10.083
66. Lawrenson K, Grun B, Gayther SA, 2012, Heterotypic Three-dimensional *In Vitro* Modeling of Stromal-epithelial Interactions during Ovarian Cancer Initiation and Progression. *J Vis Exp*, 66:e4206. https://doi.org/10.3791/4206
67. Phung YT, Barbone D, Broaddus VC, *et al*., 2011, Rapid Generation of *In Vitro* Multicellular Spheroids for the Study of Monoclonal Antibody Therapy. *J Cancer*, 2:507–14. https://doi.org/10.7150/jca.2.507
68. Kuroda Y, Wakao S, Kitada M, *et al*., 2013, Isolation, Culture and Evaluation of Multilineage-differentiating Stress-enduring (Muse) cells. *Nat Protoc*, 8:1391–415. https://doi.org/10.1038/nprot.2013.076
69. Ivascu A, Kubbies M, 2006, Rapid Generation of Single-tumor Spheroids for High-throughput Cell Function and toxicity Analysis. *J Biomol Screen*, 11:922–32. https://doi.org/10.1177/1087057106292763
70. Bilandzic M, Stenvers KL, 2014, Assessment of Ovarian Cancer Spheroid Attachment and Invasion of Mesothelial Cells in Real Time. *J Vis Exp*, 87:51655. https://doi.org/10.3791/51655
71. Huang Z, Yu P, Tang J, 2020, Characterization of Triple-Negative Breast Cancer MDA-MB-231 Cell Spheroid Model. *Onco Targets Ther*, 13:5395–405. https://doi.org/10.2147/OTT.S249756
72. Fan Y, Avci NG, Nguyen DT, *et al*., 2015, Engineering a High-Throughput 3-D *In Vitro* Glioblastoma Model. *IEEE J Transl Eng Health Med*, 3:4300108. https://doi.org/10.1109/JTEHM.2015.2410277
73. Lee D, Pathak S, Jeong JH, 2019, Design and Manufacture of 3D Cell Culture Plate for Mass Production of Cell-Spheroids. *Sci Rep*, 9:13976. https://doi.org/10.1038/s41598-019-50186-0
74. Gong X, Lin C, Cheng J, *et al*., 2015, Generation of Multicellular Tumor Spheroids with Microwell-Based Agarose Scaffolds for Drug Testing. *PLoS One*, 10:e0130348. https://doi.org/10.1371/journal.pone.0130348
75. Chao C, Ngo LP, Engelward BP, 2020, SpheroidChip:

Patterned Agarose Microwell Compartments Harboring HepG2 Spheroids are Compatible with Genotoxicity Testing. *ACS Biomater Sci Eng*, 6:2427–39. https://doi.org/10.1021/acsbiomaterials.9b01951

76. Mirab F, Kang YJ, Majd S, 2019, Preparation and Characterization of Size-controlled Glioma Spheroids Using Agarose hydrogel Microwells. *PLoS One*, 14:e0211078. https://doi.org/10.1371/journal.pone.0211078
77. Thomsen AR, Aldrian C, Bronsert P, *et al*., 2018, A Deep Conical Agarose Microwell Array for Adhesion Independent Three-dimensional Cell Culture and Dynamic Volume Measurement. *Lab Chip*, 18:179–89. https://doi.org/10.1039/C7LC00832E
78. Desroches BR, Zhang P, Choi BR, *et al*., 2012, Functional Scaffold-free 3-D Cardiac Microtissues: A Novel Model for the Investigation of Heart Cells. *Am J Physiol Heart Circ Physiol*, 302:H2031–42. https://doi.org/10.1152/ajpheart.00743.2011
79. Henslee EA, Dunlop CM, de Mel CM, *et al*., 2020, DEP-Dots for 3D Cell Culture: Low-cost, High-repeatability, Effective 3D Cell Culture in Multiple Gel Systems. *Sci Rep*, 10:14603. https://doi.org/10.1038/s41598-020-71265-7
80. Albrecht DR, Tsang VL, Sah RL, *et al*., Photo- and electropatterning of hydrogel-encapsulated living cell arrays. *Lab Chip*, 5:111–8. https://doi.org/10.1039/b406953f
81. Agarwal S, Sebastian A, Forrester LM, *et al*., 2012, Formation of Embryoid Bodies Using Dielectrophoresis. *Biomicrofluidics*, 6:24101–11. https://doi.org/10.1063/1.3699969
82. Jafari J, Han X, Palmer J, *et al*., 2019, Remote Control in Formation of 3D Multicellular Assemblies Using Magnetic Forces. *ACS Biomater Sci Eng*, 5:2532–42. https://doi.org/10.1021/acsbiomaterials.9b00297
83. Urbanczyk M, Zbinden A, Layland SL, *et al*., Controlled Heterotypic Pseudo-Islet Assembly of Human β-Cells and Human Umbilical Vein Endothelial Cells Using Magnetic Levitation. *Tissue Eng Part A*, 26:387–99. https://doi.org/10.1089/ten.TEA.2019.0158
84. Lewis NS, El Lewis E, Mullin M, *et al*., 2017, Magnetically levitated mesenchymal stem cell spheroids cultured with a collagen gel maintain phenotype and quiescence. *J Tissue Eng*, 8:2041731417704428. https://doi.org/10.1177/2041731417704428
85. Tseng H, Gage JA, Shen T, *et al*., 2015, A Spheroid Toxicity Assay Using Magnetic 3D Bioprinting and Real-time Mobile Device-based Imaging. *Sci Rep*, 5:13987. https://doi.org/10.1038/srep13987
86. Wu M, Ozcelik A, Rufo J, *et al*., 2019, Acoustofluidic Separation of Cells and Particles. *Microsyst Nanoeng*, 5:32. https://doi.org/10.1038/s41378-019-0064-3
87. Chen B, Wu Y, Ao Z, *et al*., 2019, High-throughput Acoustofluidic Fabrication of Tumor Spheroids. *Lab Chip*, 19:1755–63. https://doi.org/10.1039/C9LC00135B
88. Ota H, Miki N, 2011, Microfluidic Experimental Platform for Producing Size-controlled Three-dimensional Spheroids. *Sens Actuat A Phys*, 169:266–73. https://doi.org/10.1016/j.sna.2011.03.051
89. Hong S, Hsu HJ, Kaunas R, *et al*., 2012, Collagen Microsphere Production on a Chip. *Lab Chip*, 12:3277–80. https://doi.org/10.1039/C2LC40558J
90. Damiati S, Kompella UB, Damiati SA, *et al*., 2018, Microfluidic Devices for Drug Delivery Systems and Drug Screening. *Genes* (*Basel*), 9:103. https://doi.org/10.3390/genes9020103
91. McMillan KS, McCluskey AG, Sorensen A, *et al*., 2016, Emulsion Technologies for Multicellular Tumour Spheroid Radiation Assays. *Analyst*, 141:100–10. https://doi.org/10.1039/c5an01382h
92. Lee JM, Choi JW, Ahrberg CD, *et al*., 2020, Generation of Tumor Spheroids Using a Droplet-based Microfluidic Device for Photothermal Therapy. *Microsyst Nanoeng*, 6:52. https://doi.org/10.1038/s41378-020-0167-x
93. Lee D, Cha C, 2018, The Combined Effects of Co-Culture and Substrate Mechanics on 3D Tumor Spheroid Formation within Microgels Prepared via Flow-Focusing Microfluidic Fabrication. *Pharmaceutics*, 10:229. https://doi.org/10.3390/pharmaceutics10040229
94. Cui X, Liu Y, Hartanto Y, *et al*., 2016, Multicellular Spheroids Formation and Recovery in Microfluidics-generated Thermoresponsive Microgel Droplets. *Colloid Interface Sci Commun*, 14:4–7. https://doi.org/10.1016/j.colcom.2016.09.001
95. Zeng W, Xiang D, Fu H, 2019, Prediction of Droplet Production Speed by Measuring the Droplet Spacing Fluctuations in a Flow-Focusing Microdroplet Generator. *Micromachines*, 10:812. https://doi.org/10.3390/mi10120812
96. Kong T, Wu J, Yeung KW, *et al*., 2013, Microfluidic Fabrication of Polymeric Core-shell Microspheres for Controlled Release Applications. *Biomicrofluidics*, 7:44128. https://doi.org/10.1063/1.4819274
97. Tran TM, Lan F, Thompson CS, *et al*., 2013, From Tubes to

Drops: Droplet-based Microfluidics for Ultrahigh-throughput Biology. *J Phys D Appl Phys*, 46:114004. https://doi.org/10.1088/0022-3727/46/11/114004

98. Chan HF, Zhang Y, Ho YP, *et al*., 2013, Rapid Formation of Multicellular Spheroids in Double-emulsion Droplets with Controllable Microenvironment. *Sci Rep*, 3:3462. https://doi.org/10.1038/srep03462
99. Kim C, Chung S, Kim YE, *et al*., 2011, Generation of Core-shell Microcapsules with Three-dimensional Focusing Device for Efficient Formation of Cell Spheroid. *Lab Chip*, 11:246–52. https://doi.org/10.1039/C0LC00036A
100. Grist SM, Nasseri SS, Laplatine L, *et al*., 2019, Long-term Monitoring in a Microfluidic System to Study Tumour Spheroid Response to Chronic and Cycling Hypoxia. *Sci Rep*, 9:17782. https://doi.org/10.1038/s41598-019-54001-8
101. Wang Y, Zhao L, Tian C, *et al*., 2015, Geometrically Controlled Preparation of Various Cell Aggregates by Droplet-based Microfluidics. *Anal Methods*, 7:10040–51. https://doi.org/10.1039/C5AY02466H
102. Sun Q, Tan SH, Chen Q, *et al*., 2018, Microfluidic Formation of Coculture Tumor Spheroids with Stromal Cells As a Novel 3D Tumor Model for Drug Testing. *ACS Biomater Sci Eng*, 4:4425–33. https://doi.org/10.1021/acsbiomaterials.8b00904
103. Yazdi SR, Shadmani A, Bürgel SC, *et al*., Adding the "Heart" to Hanging Drop Networks for Microphysiological Multi-tissue Experiments. *Lab Chip*, 15:4138–47. https://doi.org/10.1039/c5lc01000d
104. Frey O, Misun PM, Fluri DA, *et al*., 2014, Reconfigurable Microfluidic Hanging Drop Network for Multi-tissue Interaction and Analysis. *Nat Commun*, 5:4250. https://doi.org/10.1038/ncomms5250
105. Wu HW, Hsiao YH, Chen CC, *et al*., 2016, A PDMS-Based Microfluidic Hanging Drop Chip for Embryoid Body Formation. *Molecules*, 21:882. https://doi.org/10.3390/molecules21070882
106. Dadgar N, Gonzalez-Suarez AM, Fattahi P, *et al*., 2020, A Microfluidic Platform for Cultivating Ovarian Cancer Spheroids and Testing their Responses to Chemotherapies. *Microsyst Nanoeng*, 6:93. https://doi.org/10.1038/s41378-020-00201-6
107. Chen SY, Hung PJ, Lee PJ, 2011, Microfluidic Array for Three-dimensional Perfusion Culture of Human Mammary Epithelial Cells. *Biomed Microdev*, 13:753–8. https://doi.org/10.1007/s10544-011-9545-3
108. Lee K, Kim C, Yang JY, *et al*., 2012, Gravity-oriented Microfluidic Device for Uniform and Massive Cell Spheroid Formation. *Biomicrofluidics*, 6:14114–47. https://doi.org/10.1063/1.3687409
109. Fiddes LK, Luk VN, Au SH, *et al*., 2012, Hydrogel Discs for Digital Microfluidics. *Biomicrofluidics*, 6:14112–211. https://doi.org/10.1063/1.3687381
110. Eydelnant IA, Li BB, Wheeler AR, 2014, Microgels on-demand. *Nat Commun*, 5:3355. https://doi.org/10.1038/ncomms4355
111. Aijian AP, Garrell RL, 2015, Digital Microfluidics for Automated Hanging Drop Cell Spheroid Culture. *J Lab Autom*, 20:283–95. https://doi.org/10.1177/2211068214562002
112. Vadivelu RK, Kamble H, Shiddiky MJ, *et al*., 2017, Microfluidic Technology for the Generation of Cell Spheroids and Their Applications. *Micromachines*, 8:94. https://doi.org/10.3390/mi8040094
113. Moshksayan K, Kashaninejad N, Warkiani ME, *et al*., 2018, Spheroids-on-a-chip: Recent Advances and Design Considerations in Microfluidic Platforms for Spheroid Formation and Culture. *Sens Actuat B Chem*, 263:151–76. https://doi.org/10.1016/j.snb.2018.01.223
114. Utama RH, Atapattu L, O'Mahony AP, *et al*., 2020, A 3D Bioprinter Specifically Designed for the High-Throughput Production of Matrix-Embedded Multicellular Spheroids. *IScience*, 23:101621. https://doi.org/10.1016/j.isci.2020.101621
115. Ling K, Huang G, Liu J, *et al*., 2015, Bioprinting-Based High-Throughput Fabrication of Three-Dimensional MCF-7 Human Breast Cancer Cellular Spheroids. *Engineering*, 1:269–74. https://doi.org/10.15302/J-ENG-2015062
116. Vinson BT, Sklare SC, Chrisey DB, 2017, Laser-based Cell Printing Techniques for Additive Biomanufacturing. *Curr Opin Biomed Eng*, 2:14–21. https://doi.org/10.1016/j.cobme.2017.05.005
117. Armon N, Greenberg E, Edri E, *et al*., 2021, Laser-Based Printing: From Liquids to Microstructures. *Adv Funct Mater*, 31:2008547. https://doi.org/10.1002/adfm.202008547
118. Hakobyan D, Médina C, Dusserre N, *et al*., 2020, Laser-assisted 3D Bioprinting of Exocrine Pancreas Spheroid Models for Cancer Initiation Study. *Biofabrication*, 12:35001. https://doi.org/10.1088/1758-5090/ab7cb8
119. Boyer CJ, Ballard DH, Barzegar M, *et al*., 2018, High-throughput Scaffold-free Microtissues through 3D Printing.

3D Print Med, 4:9.
https://doi.org/10.1186/s41205-018-0029-4

120. Swaminathan S, Clyne AM, 2020, Direct Bioprinting of 3D Multicellular Breast Spheroids onto Endothelial Networks. *J Vis Exp*, 165:61791.
https://doi.org/10.3791/61791
121. Swaminathan S, Hamid Q, Sun W, *et al*., 2019, Bioprinting of 3D Breast Epithelial Spheroids for Human Cancer Models. *Biofabrication*, 11:25003.
https://doi.org/10.1088/1758-5090/aafc49
122. Horder H, Lasheras MG, Grummel N, *et al*., 2021, Bioprinting and Differentiation of Adipose-Derived Stromal Cell Spheroids for a 3D Breast Cancer-Adipose Tissue Model. *Cells*, 10:803.
https://doi.org/10.3390/cells10040803
123. Jakab K, Norotte C, Damon B, *et al*., 2008, Tissue Engineering by Self-assembly of Cells Printed into Topologically Defined Structures. *Tissue Eng Part A*, 14:413–21.
https://doi.org/10.1089/tea.2007.0173
124. Campos DF, Lindsay CD, Roth JG, *et al*., 2020, Bioprinting Cell-and Spheroid-Laden Protein-Engineered Hydrogels as Tissue-on-Chip Platforms. *Front Bioeng Biotechnol*, 8:374.
https://doi.org/10.3389/fbioe.2020.00374
125. Vinson BT, Phamduy TB, Shipman J, *et al*., 2017, Laser Direct-write Based Fabrication of a Spatially-defined, Biomimetic Construct as a Potential Model for Breast Cancer Cell Invasion into Adipose Tissue. *Biofabrication*, 9:25013.
https://doi.org/10.1088/1758-5090/aa6bad
126. Chen K, Jiang E, Wei X, *et al*., 2021, The Acoustic Droplet Printing of Functional Tumor Microenvironments. *Lab Chip*, 21:1604–12.
https://doi.org/10.1039/D1LC00003A
127. Moldovan NI, Hibino N, Nakayama K, 2017, Principles of the Kenzan Method for Robotic Cell Spheroid-Based Three-Dimensional Bioprinting. *Tissue Eng Part B Rev*, 23:237–44.
https://doi.org/10.1089/ten.TEB.2016.0322
128. Arai K, Murata D, Verissimo AR, *et al*., 2018, Fabrication of Scaffold-free Tubular Cardiac Constructs Using a Bio-3D Printer. *PLoS One*, 13:e0209162.
https://doi.org/10.1371/journal.pone.0209162
129. LaBarge W, Morales A, Pretorius D, *et al*., 2019, Scaffold-Free Bioprinter Utilizing Layer-By-Layer Printing of Cellular Spheroids. *Micromachines*, 10:570.
https://doi.org/10.3390/mi10090570
130. Murata D, Arai K, Nakayama K, 2020, Scaffold-Free Bio-3D Printing Using Spheroids as "Bio-Inks" for Tissue (Re-) Construction and Drug Response Tests. *Adv Healthc Mater*, 9:e1901831.
https://doi.org/10.1002/adhm.201901831
131. van Pel DM, Harada K, Song D, *et al*., 2018, Modelling Glioma Invasion Using 3D Bioprinting and Scaffold-free 3D Culture. *J Cell Commun Signal*, 12:723–30.
https://doi.org/10.1007/s12079-018-0469-z
132. Kizawa H, Nagao E, Shimamura M, *et al*., 2017, Scaffold-free 3D Bio-printed Human Liver Tissue Stably Maintains Metabolic Functions Useful for Drug Discovery. *Biochem Biophys Reports*, 10:186–91.
https://doi.org/10.1016/j.bbrep.2017.04.004
133. Ip BC, Cui F, Tripathi A, *et al*., 2016, The Bio-gripper: A Fluid-driven Micro-Manipulator of Living Tissue Constructs for Additive Bio-manufacturing. *Biofabrication*, 8:25015.
https://doi.org/10.1088/1758-5090/8/2/025015
134. Blakely AM, Manning KL, Tripathi A, *et al*., 2015, Bio-Pick, Place, and Perfuse: A New Instrument for Three-Dimensional Tissue Engineering. *Tissue Eng Part C Methods*, 21:737–46.
https://doi.org/10.1089/ten.TEC.2014.0439
135. Ayan B, Heo DN, Zhang Z, *et al*., 2020., Aspiration-assisted Bioprinting for Precise Positioning of Biologics. *Sci Adv*, 6:eaaw5111.
https://doi.org/10.1126/sciadv.aaw5111
136. Ayan B, Celik N, Zhang Z, *et al*., 2020, Aspiration-assisted Freeform Bioprinting of Pre-fabricated Tissue Spheroids in a Yield-stress Gel. *Commun Phys*, 3:183.
https://doi.org/10.1038/s42005-020-00449-4
137. Daly AC, Davidson MD, Burdick JA, 2021, 3D Bioprinting of High Cell-density Heterogeneous Tissue Models through Spheroid Fusion within Self-healing Hydrogels. *Nat Commun*, 12:753.
https://doi.org/10.1038/s41467-021-21029-2
138. Norotte C, Marga FS, Niklason LE, *et al*., 2009, Scaffold-free Vascular Tissue Engineering Using Bioprinting. *Biomaterials*, 30:5910–7.
https://doi.org/10.1016/j.biomaterials.2009.06.034
139. Bulanova EA, Koudan EV, Degosserie J, *et al*., 2017, Bioprinting of a Functional Vascularized Mouse Thyroid Gland Construct. *Biofabrication*, 9:34105.
https://doi.org/10.1088/1758-5090/aa7fdd
140. Kozaki S, Moritoki Y, Furukawa T, *et al*., 2020, Additive Manufacturing of Micromanipulator Mounted on a Glass Capillary for Biological Applications. *Micromachines*, 11:174.
https://doi.org/10.3390/mi11020174
141. Zhuang P, An J, Tan LP, *et al*., 2018, The Current Status of 3D Bioprinting for Neural Tissue Models. 2018:183–8.

https://doi.org/10.25341/D4688F

142. Zhuang P, Ng WL, An J, *et al*., 2019, Layer-by-layer Ultraviolet Assisted Extrusion-based (UAE) Bioprinting of Hydrogel Constructs with High Aspect Ratio for Soft Tissue Engineering Applications. *PLoS One*, 14:e0216776. https://doi.org/10.1371/journal.pone.0216776
143. Li X, Liu B, Pei B, *et al*., 2020, Inkjet Bioprinting of Biomaterials. *Chem Rev*, 120:10793–833. https://doi.org/10.1021/acs.chemrev.0c00008
144. Koch L, Gruene M, Unger C, *et al*., 2013, Laser Assisted Cell Printing. *Curr Pharm Biotechnol*, 14:91–7.
145. Grigoryan B, Sazer DW, Avila A, *et al*., 2021, Development, Characterization, and Applications of Multi-Material Stereolithography Bioprinting. *Sci Rep*, 11:3171. https://doi.org/10.1038/s41598-021-82102-w
146. Matai I, Kaur G, Seyedsalehi A, *et al*., 2020, Progress in 3D Bioprinting Technology for Tissue/Organ Regenerative Engineering. *Biomaterials*, 226:119536. https://doi.org/10.1016/j.biomaterials.2019.119536
147. Murphy SV, De Coppi P, Atala A, 2020, Opportunities and Challenges of Translational 3D Bioprinting. *Nat Biomed Eng*, 4:370–80. https://doi.org/10.1038/s41551-019-0471-7
148. Cui X, Li J, Hartanto Y, *et al*., 2020, Advances in Extrusion 3D Bioprinting: A Focus on Multicomponent Hydrogel-Based Bioinks. *Adv Healthc Mater*, 9:1901648. https://doi.org/10.1002/adhm.201901648
149. Zhuang P, Greenberg Z, He M, 2021, Biologically Enhanced Starch Bio-Ink for Promoting 3D Cell Growth. *Adv Mater Technol*, 2021:2100551. https://doi.org/10.1002/admt.202100551
150. McCormack A, Highley CB, Leslie NR, *et al*., 2020, 3D Printing in Suspension Baths: Keeping the Promises of Bioprinting Afloat. *Trends Biotechnol*, 38:584–93. https://doi.org/10.1016/j.tibtech.2019.12.020
151. Hermida MA, Kumar JD, Schwarz D, *et al*., 2020, Three Dimensional *In Vitro* Models of Cancer: Bioprinting Multilineage Glioblastoma Models. *Adv Biol Regul*, 75:100658. https://doi.org/10.1016/j.jbior.2019.100658
152. Dai X, Liu L, Ouyang J, *et al*., 2017, Coaxial 3D Bioprinting of Self-assembled Multicellular Heterogeneous Tumor Fibers. *Sci Rep*, 7:1457. https://doi.org/10.1038/s41598-017-01581-y
153. Wang X, Li X, Dai X, *et al*., 2018, Coaxial Extrusion Bioprinted Shell-core Hydrogel Microfibers Mimic Glioma Microenvironment and Enhance the Drug Resistance of Cancer Cells. *Colloids Surf B Biointerfaces*, 171:291–9. https://doi.org/10.1016/j.colsurfb.2018.07.042
154. Yi HG, Jeong YH, Kim Y, *et al*., 2019, A Bioprinted Human-glioblastoma-on-a-Chip for the Identification of Patient-specific Responses to Chemoradiotherapy. *Nat Biomed Eng*, 3:509–19. https://doi.org/10.1038/s41551-019-0363-x
155. Wang X, Li X, Ding J, *et al*., 2021, 3D Bioprinted Glioma Microenvironment for Glioma Vascularization. *J Biomed Mater Res Part A*, 109:915–25. https://doi.org/10.1002/jbm.a.37082
156. Wang X, Li X, Dai X, *et al*., 2018, Bioprinting of Glioma Stem Cells Improves their Endotheliogenic Potential. *Colloids Surf B Biointerfaces*, 171:629–37. https://doi.org/10.1016/j.colsurfb.2018.08.006
157. Lee VK, Dai G, Zou H, *et al*., 2015, Generation of 3-D Glioblastoma-vascular Niche Using 3-D Bioprinting. In: 2015 41st Annual Northeast Biomedical Engineering Conference, p1-2. https://doi.org/10.1109/NEBEC.2015.7117111
158. Wang X, Zhang X, Dai X, *et al*., 2018, Tumor-like Lung Cancer Model Based on 3D Bioprinting. *3 Biotech*, 8:501. https://doi.org/10.1007/s13205-018-1519-1
159. Zhou X, Zhu W, Nowicki M, *et al*., 2016, 3D Bioprinting a Cell-Laden Bone Matrix for Breast Cancer Metastasis Study. *ACS Appl Mater Interfaces*, 8:30017–26. https://doi.org/10.1021/acsami.6b10673
160. Zhu W, Holmes B, Glazer RI, *et al*., 2016, 3D Printed Nanocomposite Matrix for the Study of Breast Cancer Bone Metastasis. *Nanomedicine*, 12:69–79. https://doi.org/10.1016/j.nano.2015.09.010
161. Han S, Kim S, Chen Z, *et al*., 2020, 3D Bioprinted Vascularized Tumour for Drug Testing. *Int J Mol Sci*, 21:2993. https://doi.org/10.3390/ijms21082993
162. Smits IP, Blaschuk OW, Willerth SM, 2020, Novel N-cadherin Antagonist Causes Glioblastoma Cell Death in a 3D Bioprinted Co-culture Model. *Biochem Biophys Res Commun*, 529:162–8. https://doi.org/10.1016/j.bbrc.2020.06.001
163. Mironov V, Visconti RP, Kasyanov V, *et al*., 2009, Organ Printing: Tissue Spheroids as Building Blocks. *Biomaterials*, 30:2164–74. https://doi.org/10.1016/j.biomaterials.2008.12.084
164. Ahmad T, Shin HJ, Lee J, *et al*., 2018, Fabrication of *In Vitro* 3D Mineralized Tissue by Fusion of Composite Spheroids Incorporating Biomineral-coated Nanofibers and Human Adipose-derived Stem Cells. *Acta Biomater*, 74:464–77.

https://doi.org/10.1016/j.actbio.2018.05.035

165. Kelm JM, Lorber V, Snedeker JG, *et al*., 2010, A Novel Concept for Scaffold-free Vessel Tissue Engineering: Self-assembly of Microtissue Building Blocks. *J Biotechnol*, 148:46–55. https://doi.org/10.1016/j.jbiotec.2010.03.002
166. Birey F, Andersen J, Makinson CD, *et al*., 2017, Assembly of Functionally Integrated human Forebrain Spheroids. *Nature*, 545:54–9. https://doi.org/10.1038/nature22330
167. Kato-Negishi M, Morimoto Y, Onoe H, *et al*., 2013, Millimeter-Sized Neural Building Blocks for 3D Heterogeneous Neural Network Assembly. *Adv Healthc Mater*, 2:1564–70. https://doi.org/10.1002/adhm.201300052
168. Fleming PA, Argraves WS, Gentile C, *et al*., 2010, Fusion of Uniluminal Vascular Spheroids: A Model for Assembly of Blood Vessels. *Dev Dyn*, 239:398–406. https://doi.org/10.1002/dvdy.22161
169. Dean DM, Napolitano AP, Youssef J, *et al*., 2007, Rods, Tori, and Honeycombs: The Directed Self-assembly of Microtissues with Prescribed Microscale Geometries. *FASEB J*, 21:4005–12. https://doi.org/10.1096/fj.07-8710com
170. Luo J, Meng J, Gu Z, *et al*., 2019, Topography-Induced Cell Self-Organization from Simple to Complex Aggregates. *Small*, 15:1900030. https://doi.org/10.1002/smll.201900030
171. Olsen TR, Mattix B, Casco M, *et al*., 2015, Manipulation of Cellular Spheroid Composition and the Effects on Vascular Tissue Fusion. *Acta Biomater*, 13:188–98. https://doi.org/10.1016/j.actbio.2014.11.024
172. Mattix B, Olsen TR, Gu Y, *et al*., 2014, Biological Magnetic Cellular Spheroids as Building Blocks for Tissue Engineering. *Acta Biomater*, 10:623–9. https://doi.org/10.1016/j.actbio.2013.10.021
173. Whatley BR, Li X, Zhang N, *et al*., 2014, Magnetic-directed Patterning of cell Spheroids. *J Biomed Mater Res A*, 102:1537–47. https://doi.org/10.1002/jbm.a.34797
174. Lin RZ, Chu WC, Chiang CC, *et al*., 2008, Magnetic Reconstruction of Three-Dimensional Tissues from Multicellular Spheroids. *Tissue Eng Part C Methods*, 14:197–205. https://doi.org/10.1089/ten.tec.2008.0061
175. Bratt-Leal AM, Kepple KL, Carpenedo RL, *et al*., 2011, Magnetic Manipulation and Spatial Patterning of Multi-cellular Stem Cell Aggregates. *Integr Biol* (*Camb*), 3:1224–32. https://doi.org/10.1039/c1ib00064k
176. Fayol D, Frasca G, Le Visage C, *et al*., 2013, Use of Magnetic Forces to Promote Stem Cell Aggregation During Differentiation, and Cartilage Tissue Modeling. *Adv Mater*, 25:2611–6. https://doi.org/10.1002/adma.201300342
177. Chen P, Güven S, Usta OB, *et al*., 2015, Biotunable Acoustic Node Assembly of Organoids. *Adv Healthc Mater*, 4:1937–43. https://doi.org/10.1002/adhm.201500279
178. Parfenov VA, Koudan EV, Krokhmal AA, *et al*., 2020, Biofabrication of a Functional Tubular Construct from Tissue Spheroids Using Magnetoacoustic Levitational Directed Assembly. *Adv Healthc Mater*, 9:2000721. https://doi.org/10.1002/adhm.202000721
179. Heinrich MA, Bansal R, Lammers T, *et al*., 2019, 3D-Bioprinted Mini-Brain: A Glioblastoma Model to Study Cellular Interactions and Therapeutics. *Adv Mater*, 31:e1806590. https://doi.org/10.1002/adma.201806590
180. Tang M, Xie Q, Gimple RC, *et al*., 2020, Three-dimensional Bioprinted Glioblastoma Microenvironments Model Cellular Dependencies and Immune Interactions. *Cell Res*., 30:833–53. https://doi.org/10.1038/s41422-020-0338-1
181. Weis SM, Cheresh DA, 2011, Tumor Angiogenesis: Molecular Pathways and Therapeutic Targets. *Nat Med*, 17:1359–70. https://doi.org/10.1038/nm.2537
182. Dey M, Ayan B, Yurieva M, *et al*., 2021, Studying Tumor Angiogenesis and Cancer Invasion in a Three-Dimensional Vascularized Breast Cancer Micro-Environment. *Adv Biol*, 2021:e2100090. https://doi.org/10.1002/adbi.202100090
183. Meng F, Meyer CM, Joung D, *et al*., 2019, 3D Bioprinted *In Vitro* Metastatic Models via Reconstruction of Tumor Microenvironments. *Adv Mater*, 31:e1806899. https://doi.org/10.1002/adma.201806899
184. Maloney E, Clark C, Sivakumar H, *et al*., 2020, Immersion Bioprinting of Tumor Organoids in Multi-Well Plates for Increasing Chemotherapy Screening Throughput. *Micromachines*, 11:208. https://doi.org/10.3390/mi11020208
185. Li Y, Zhang T, Pang Y, *et al*., 2019, 3D Bioprinting of Hepatoma Cells and application with microfluidics for pharmacodynamic test of Metuzumab. *Biofabrication*, 11:34102. https://doi.org/10.1088/1758-5090/ab256c
186. Sun L, Yang H, Wang Y, *et al*., 2020, Application of a 3D Bioprinted Hepatocellular Carcinoma Cell Model in

Antitumor Drug Research. *Front Oncol*, 10:878. https://doi.org/10.3389/fonc.2020.00878

187. Zhang J, Chen F, He Z, *et al*., 2016, A Novel Approach for Precisely Controlled Multiple Cell Patterning in Microfluidic Chips by Inkjet Printing and the Detection of Drug Metabolism and Diffusion. *Analyst*, 141:2940–7. https://doi.org/10.1039/C6AN00395H
188. Xie F, Sun L, Pang Y, *et al*., 2021, Three-dimensional Bio-printing of Primary Human Hepatocellular Carcinoma for Personalized Medicine. *Biomaterials*, 265:120416. https://doi.org/10.1016/j.biomaterials.2020.120416
189. Skylar-Scott MA, Uzel SG, Nam LL, *et al*., 2019, Biomanufacturing of Organ-Specific Tissues with High Cellular Density and Embedded Vascular Channels. *Sci Adv*, 5:eaaw2459. https://doi.org/10.1126/sciadv.aaw2459
190. Lee J, Oh SJ, An SH, *et al*., 2020, Machine Learning-based Design Strategy for 3D Printable Bioink: Elastic Modulus and Yield Stress Determine Printability. *Biofabrication*, 12:35018. https://doi.org/10.1088/1758-5090/ab8707
191. Yin R, Luo Z, Zhuang P, *et al*., 2021, VirPreNet: A Weighted Ensemble Convolutional Neural Network for the Virulence Prediction of Influenza A Virus Using All Eight Segments. *Bioinformatics*, 37:737–43. https://doi.org/10.1093/bioinformatics/btaa901
192. Yin R, Zhou X, Rashid S, *et al*., 2020, HopPER: An Adaptive Model for Probability Estimation of Influenza Reassortment through Host Prediction. *BMC Med Genomics*, 13:9. https://doi.org/10.1186/s12920-019-0656-7
193. Lazzari G, Nicolas V, Matsusaki M, *et al*., 2018, Multicellular Spheroid Based on a Triple Co-culture: A Novel 3D Model to Mimic Pancreatic Tumor Complexity. *Acta Biomater*, 78:296–307. https://doi.org/10.1016/j.actbio.2018.08.008
194. Meier-Hubberten JC, Sanderson MP, 2019, Establishment and Analysis of a 3D Co-Culture Spheroid Model of Pancreatic Adenocarcinoma for Application in Drug Discovery. *Methods Mol Biol*, 1953:163–79. https://doi.org/10.1007/978-1-4939-9145-7_11
195. De Moor L, Merovci I, Baetens S, *et al*., 2018, High-throughput Fabrication of Vascularized Spheroids for Bioprinting. *Biofabrication*, 10:35009. https://doi.org/10.1088/1758-5090/aac7e6
196. Noguchi R, Nakayama K, Itoh M, *et al*., 2016, Development of a Three-Dimensional Pre-vascularized Scaffold-free Contractile Cardiac Patch for Treating Heart Disease. *J Heart Lung Transplant*, 35:137–45. https://doi.org/10.1016/j.healun.2015.06.001